MAPPING WETLANDS USING GIS AND REMOTE SENSING TECHNIQUES, A CASE STUDY OF WETLANDS IN GREATER ACCRA, GHANA

Michael Kofi Mborah Amoah

A Thesis

Submitted to the Graduate College of Bowling Green State University in partial fulfillment of the requirements for the degree of

MASTER OF SCIENCE

December 2022

Committee:

Peter Gorsevski, Committee Chair

Kefa Otiso

Yu Zhou

ABSTRACT

Peter Gorsevski, Committee Chair

The goal of this study is to explore land use and land cover (LULC trends in Greater Accra Metropolitan Area (GAMA, a highly urbanized coastal region in Ghana by analyzing historical change rates and forecasting future scenarios. As industrialization and basic anthropological necessities increase in the region, natural land resources, specifically wetlands, are undergoing adverse changes. With the help of Modules for Land Use Change Evaluation (MOLUSCE which is a plugin in QGIS, the study identifies land-use changes in GAMA for 2002, 2013, and 2020 as well as forecasts and establishes potential land-use changes in 2030 and 2040. The presented approach incorporates well-known algorithms such as artificial neural networks (ANN for computing transition potential maps coupled with cellular automata (CA simulation. To analyze their impact on LULC between 2002 and 2013, five criteria were used in the CA-ANN framework, including elevation, slope, distance from roads, distance from towns, and distance from rivers. The validation of simulated LULC maps for 2020 indicates a good level of accuracy, with a kappa value of 0.70 and a correctness percentage of 78.50%. The future scenarios between 2020 and 2040 indicate that urban development and sprawl are expected to increase annually at a dynamic degree rate of 0.86% at the expense of natural land covers such as wetlands and vegetation. The major road network in GAMA spearheads the growth of developed areas, while slope and elevation act as constraints. A high ratio of impervious to pervious surfaces confirms the rapid urbanization of the area. Urbanization is likely to have a more detrimental effect on natural habitats in the near future less so in the distant future. This study emphasizes the importance of establishing appropriate urban planning policies and management methods for sustainable environmental conservation.

I dedicate this to my mother Georgina, my father Francis, and my wonderful siblings Rita, Abigail, and Francisca. Thank you for all your love, support, and encouragement.

ACKNOWLEDGMENTS

I would like to thank my advisor, Dr. Peter Gorsevski, for his guidance, support, knowledge, and patience, as he has spent many hours assisting me with this thesis, responding promptly to all my inquiries. In addition, I would like to express my thanks to Dr. Kefa Otiso and Dr. Yu Zhou for their guidance, advice, and support for this thesis research.

It is my pleasure to thank Nana Yaw Osei for his review and guidance, as well as Emmanuel Cobbinah for his support. Also, a big thanks to the faculty and students of the Geology program of the School of Earth, Environment, and Society at Bowling Green State University for introducing me to a new field of study.

Lastly, I would like to thank my family and friends both abroad and here in the US for their love and support over the past two and a half years, as I pursued my graduate degree away from home. You all made it possible for me to finish this project. Please accept my sincere thanks.

TABLE OF CONTENTS

Page

INTRODUCTION

Wetlands provide important ecosystem services such as habitats for wildlife (Knight et al., 2001), mitigation of floods (Pattison-Williams et al., 2018), and climate moderation (Mitsch et al., 2013). Over the last century, wetlands have been polluted and have declined significantly due to rapid land cover change around the world (Zedler & Kercher, 2005). The principal threat to wetlands is attributed to anthropogenic factors such as urbanization, road and building construction, removal of vegetation for firewood and farmland creation, water consumption, pollution, and the introduction of invasive species among others (Ekumah et al., 2020; Sun et al., 2020). In developed countries, the valuable services that wetlands provide are generally well understood. Therefore, conservation and restoration efforts have been implemented to preserve them (Niu et al., 2012; Uuemaa et al., 2018). Contrarily, the implementation of restoration efforts in developing countries has been much more challenging due to pressing needs for housing, increased food production, and other necessities.

Specifically, massive areas of Ramsar wetlands (https://www.ramsar.org) which is an international program that preserves wetlands have been affected by urbanization globally. For example, an assessment of land cover changes between 1985 and 2017 at three Ramsar sites in Ghana suggested significant wetland losses at a rate of change between 2.6 % and 3.6 % annually (Ekumah et al. 2020). The study infers that urban expansion driven by the increased demand for dwellings was the chief factor that contributed to the destruction of wetlands. Also, a number of studies are pinpointing specific regions such as the Greater Accra Region of Ghana (the nation's economic hub) that are experiencing very high rates of urban sprawl (Osei et al., 2013; Stemn & Agyapong, 2014). Although Ghana has been a signatory of the Ramsar Convention since 1988 which obligates it to conserve its wetlands, it has lagged behind properly managing and conserving its wetlands because of many factors including a lack of information on the extent and distribution of wetland resources (Ministry of Lands and Forestry, 1999; Job et al., 2020). Thus, identifying and mapping Ghana's wetlands as well as understanding how they are impacted by anthropogenic activities are key steps in building a framework to understand, manage, rehabilitate, and conserve these ecosystems (Ozesmi & Bauer, 2002).

Wetlands are defined as saturated ecosystems "areas with water long enough to promote wetland or aquatic processes as indicated by poorly drained soils, hydrophytic vegetation, and various kinds of biological activities that are adapted to a wet environment" (National Wetland Working Group, 1997). Field surveys have been the traditional approach for detailed wetland mapping which involves delineation using field guides (Mackenzie & Moran, 2004) and tools for wetland sampling (Tiner, 1999). The identification of wetlands by field-based methods often relies on vegetation characteristics and species dominance that are adapted to the environmental conditions of wetlands-hydrophytes. However, a major shortcoming of this method is that the dominance of hydrophytes and their composition and distribution in wetlands changes with decreasing soil wetness. This leads to the need for an additional examination of the hydrology and presence of hydric soils, as vegetation characteristics alone are insufficient for mapping wetlands (Tiner, 1999). Moreover, field-based methods are costly in terms of time, labor, and resources and can best be applied to wetlands with small geographic extents which are easily accessible (Moser et al., 2016).

Recent developments in remote sensing (RS) and geographic information systems (GIS) techniques provide a new modeling framework that enables widespread applicability and advancements for identifying and mapping different earth features, including wetlands (Ozesmi & Bauer, 2002; Kumar & Sinha, 2014). RS-based methods are more cost-effective than field surveys and they provide better observational capabilities at the satellite, aerial, drone, or unmanned aerial vehicle (UAV), and ground levels. At different scales, a variety of airborne approaches have been used for mapping wetlands using RS data from platforms like Landsat, Sentinel, ALOS PALSAR, and LiDAR (Mahdianpari et al., 2017; Wu & Lane, 2017; Niculescu et al., 2020). However, RS methods do not rule out field-based methods rather they reduce the need for detailed field data and provide a synoptic view for mapping and monitoring large geographic areas (Mahdavi et al., 2018). In fact, the field-based methods or *in situ* ground observations are complementary tools that support RS classification, accuracy, and assessment methods (Rundquist et al., 2001; Ozesmi & Bauer, 2002; Dronova, 2015).

Satellites such as the Landsat and Sentinel provide open access to data that can be processed over large areas and at regular time periods (Gabrielsen et al., 2016). Most wetland data present today at the global and national levels are derived from satellites (Lehner & Döll, 2004; Niu et al., 2012). The multispectral sensors acquire information at different spectral bands in the visible, near-infrared, mid-infrared, and thermal infrared regions of the electromagnetic spectrum. Thus, they are useful in classifying and separating wetlands from other land cover features (Arzandeh & Wang, 2002; Gosselin et al., 2014; Gallant, 2015). Several indices such as the normalized difference vegetation index (NDVI), normalized difference built-up index (NDBI), and modified normalized difference water index (MNDWI) can be derived from optical images and incorporated into wetland delineation models which are often used for land use and land cover (LULC) assessment (Li & Chen, 2005; Sun et al., 2020).

LULC changes are an effective technique that is employed in diverse disciplines in the monitoring, assessment, evaluation, mapping, and prediction of the impact of change on ecosystems at various spatio-temporal scales (Halmy et al., 2015; Balogun & Ishola, 2017; Aboelnour & Engel, 2018).

With the global increase in urban areas, a proper understanding of past and extant scenarios of LULC changes provides managers the opportunity to evaluate past management decisions and allow them to review land management plans that can alleviate anthropogenic-induced impacts on the environment (Liou et al., 2017; Faisal & Khan, 2017). Urbanization is most prevalent in developing countries, where rapid socio-economic and infrastructure growth has led to extensive LULC changes that adversely affect environmental sustainability (Abdullah et al., 2019). Ghana, in particular, has urbanized rapidly, and now has a large proportion of its population living in urban areas. In 2010, close to half of the nation's population was estimated to be urban, a figure that is projected to reach seventy percent (70%) by 2050 (Ghana Statistical Service, 2010). LULC change studies have identified urban growth as the primary cause of fragmentation and eventual loss of important ecosystems like wetlands (Awotwi et al., 2019; Ekumah et al., 2020). Thus, monitoring LULC changes is necessary for devising proper management practices that are geared towards biodiversity conservation and environmental sustainability (Ekumah et al., 2020).

LULC change detection techniques rely on the use of RS and GIS techniques which are important sources of information for various spatial decision support systems. The use of these techniques allows for timely and detailed views of land cover changes and analytics, providing a useful approach for monitoring the dynamics and spatial distribution of urban areas (Tian et al., 2014; Hua et al., 2017; Kafy et al., 2020). For example, Adade et al. (2017), used RS and GIS techniques to assess LULC changes in the Songor Ramsar Site in the southeastern coastal savanna of Ghana. The Songor Ramsar Site provides habitat and breeding grounds for turtles and several bird species, such as the black-winged stilt. According to the study, there was considerable habitat loss and fragmentation of the site, caused mostly by deforestation, sustained by human settlements, agriculture, and infrastructure development. LULC is thus critical to understanding environmental change dynamics, past conditions, monitoring, planning, management, forming policies, and integrating RS and GIS.

Literature provides various methods for predicting LULC changes. These methods differ depending on the purpose, approach, scale, geographic areas of interest, assumptions, and the source and type of data used (Michetti & Zampieri, 2014). Commonly used LULC mapping techniques are artificial neural network (ANN) (Prasad et al., 2017; Shihab et al., 2020), random forest (RF) (Christovam et al., 2019; Shihab et al., 2020), spectral angle mapper (SAM) (Christovam et al., 2019), support vector machine (SVM) (Otukei & Blaschke, 2010; Prasad et al., 2017; Christovam et al., 2019), maximum likelihood (ML) (Manandhar et al., 2009; Otukei & Blaschke, 2010; Allam et al., 2019), and decision tree (DT) (Otukei & Blaschke, 2010; Hua et al., 2017; Yang et al., 2017).

The DT classifier or classification and regression trees (CART) algorithm is a nonparametric technique used for predictive modeling in the field of machine learning. The continuous or categorical dependent variable in CART is explained by multiple independent variables (i.e., vegetation indices or GIS layers). Its predictive models are produced by recursive partitioning of the data space and fitting a simple model that can be represented graphically as a decision tree. The structure of the decision tree consists of root nodes, internal nodes, and leaf nodes. The root node is the beginning node or the dataset used in the predictive model, the internal node is the decision-making node that splits the data into subgroups (i.e., homogeneous objects) and the leaf node is the terminal node that holds the decision. In the recursive process, the division increases in homogeneity until each node represents a class (Hua et al., 2017; Mahdavi et al., 2018). Using Landsat data, Otukei & Blaschke (2010) examined DT, ML, and SVM-based strategies for assessing land cover change and found that DT-based methods outperformed the others.

Other popular LULC approaches include empirical and statistical models, such as Markov chains (MC), regression models, cellular automata (CA), agent-based models (ABM), system dynamic models, and integrated models such as the conversion of land use and its effects (CLUE) model (Guan et al., 2011). The CA model is one preferred approach to simulate spatio-temporal urban expansion and it addresses many environmental problems (Liu et al., 2017; Alam et al., 2021). The CA is characterized by cellular space which is the spatial representation of two-dimensional lattice or cells that represent land uses, neighborhood, and transition rules. Indeed, the transition rules determine the state of a cell in the next generation based on the current state and the state of the neighborhood (i.e., Von Neumann and Moore neighborhood) (Santé et al., 2010; Losiri et al., 2016; Kourosh Niya et al., 2020; Gharaibeh et al., 2020). For example, the slope, land use, exclusion, urban, transportation, and hillshade (SLEUTH) is a land-use change model based on the CA model that applies transition rules to the states of gridded cells (Silva & Clarke, 2002; Jayasinghe et al., 2021). The calibration process in SLEUTH is achieved based on the comparison of simulated results and observed historical data or based on an expert's hypothesis (Guan et al., 2005). Although CA model applications have increased due to its simplicity, flexibility, and ability to integrate processes spatially and temporally, several limitations exist in the quantitative aspect of the CA model, such as the inability to simulate driving forces (Santé et al., 2010; Aburas et al., 2016; Alam et al., 2021). These limitations are often managed by coupling CA models with other quantitative models such as the MC (Santé et al., 2010; Arsanjani et al., 2013; Aburas et al., 2016).

MC is a stochastic approach used widely in urban growth modeling suited for short-term projections with a one-step transition, that is the probability of transitioning from one state to another in a single step (Rendana et al., 2015; Gharaibeh et al., 2020). However, multi-step transitioning can easily be simulated by combining the capability of a cellular automata Markov chain (CA-MC) model to predict changes in LULC (Yuan et al., 2015; Kafy et al., 2021, Halmy et al., 2015; El-Tantawi et al., 2019; Addae & Oppelt, 2019; Abbas et al., 2021).

Some of the CA-MC frameworks derive transition probability matrices by cross-tabulation of land cover changes with integrated driving forces (i.e., factors such as slope, elevation, and distance from roads) from algorithms such as ANN (Losiri et al., 2016; Gharaibeh et al., 2020; Sobhani et al., 2021, Kourosh Niya et al., 2020). For example, ANNs are biologically inspired computer models by the human brain and nervous system that allow the learning of relationships and concepts for simulating complicated systems such as geospatial dynamic phenomena (Li & Yeh, 2002; Mohammady et al., 2014; Alam et al., 2021). In addition to capturing nonlinear relationships between factors, ANNs can be used to analyze complex patterns such as urban growth and land-use change. The back propagation (BP) is the most widely used algorithm which consists of an input layer, an output layer, and one or more hidden layers where weights are randomly generated, and then the variances between expected and calculated outputs are calculated and adjusted according to a generalized delta rule. This iterative process is continuous until weights are optimized and output error is minimized (Guan et al., 2005; Gharaibeh et al., 2020). The advantage of ANN is that they directly illustrate the effects of each driving factor during the simulation and specify which factors have a greater effect for a clearer understanding of land changes (Park et al., 2011; Gharaibeh et al., 2020). A CA-ANN model is a reliable method for predicting potential future LULC and plays an essential role in land use planning and management (Pijanowski et al., 2002; Guan et al., 2005).

In Ghana, although there is an increasing interest in the application of accurate wetland mapping, relatively few studies have investigated the areas at risk and the important drivers of wetland changes. This study uses the integrated CA-ANN modeling approach in the Greater Accra Metropolitan Area (GAMA), to identify LULC changes for the period 2002 - 2020 as well as predict potential changes in LULC for 2030 and 2040, with a particular interest in the impacts of urban growth on wetlands in the region. This research can provide useful results for planning and developing sustainable land and wetland management policies.

Objectives

The purpose of this research is to ascertain the changes wetlands have undergone over the years in GAMA, what drives these changes, and finally, predict their future extent based on transitional trends. The specific objectives are: (i) to delineate wetlands and implement classification analysis of temporal land cover changes; (ii) to simulate and predict future potential land-use changes.

The first objective seeks to display and determine wetland extent from LULC maps created from classified spatio-temporal satellite images. LULC maps are generated from optical bands from satellite images as well as indices derived from them using the DT classification algorithm. The second objective predicts potential land-use changes by CA-ANN approach and assesses the potential environmental risks associated with continued LULC changes.

MATERIALS AND METHODOLOGY

Study Area

The Greater Accra Metropolitan Area (GAMA) is the area of focus in this study. GAMA lies along the Atlantic coast of Ghana in West Africa (Figure 1). It is the political and economic center of the country. GAMA has a population of about four million people (Ministry of Gender, Children and Social Protection, 2014) which is growing at a rate of 4.4% per year. The study area is the most urbanized in the country with more than 90% of its population living in urban areas (Osei et al., 2013). The topography of the region varies from flat to gentle slopes with a few isolated hills (Njomaba et al., 2021).

The region lies within the dry equatorial climatic zone with two rainy seasons. The first rainy season begins in March and ends in July while the second begins in September and ends in November. The region experiences a mean average temperature of 26.8 °C (Njomaba et al., 2021). Severe perennial floods are a persistent problem in this region due to factors such as urbanization with its detrimental effects on the drainage system and important flood mitigation ecosystems like wetlands (Asumadu-Sarkodie et al., 2015).

There are two coastal urban wetlands in the study area; the Densu Delta and the Sakumo Ramsar sites. Ramsar sites Densu and Sakumo are being depleted at an annual rate of 2.6 and 3.6%, respectively (Ekumah et al., 2020). The region has coastal savannah and inland forest areas in the Ga districts (Osei et al., 2013).

Datasets

The multispectral Landsat imagery (Table 1) was acquired from the USGS Global Visualization Viewer (GloVis) (https://glovis.usgs.gov/) while the Global Digital Elevation Model (GDEM) data were obtained from NASA's EarthData platform (https://search.earthdata.nasa.gov/search/). The Landsat images were acquired from December to January, during the dry season, to obtain images with fewer clouds and avoid extreme variations in land cover reflectance. At the preprocessing stage, atmospheric corrections were performed by the Quick Atmospheric Correction (QUAC) which is often applied for conditions such as thick haze, smoke, or under cloud cover after datasets acquired were transformed from DN values to radiance. Other auxiliary datasets including vector data for roads, water bodies, administrative boundaries, and towns were provided by the University of Ghana. The UTM (Universal Transverse Mercator) projection system, World Geodetic System 1984 (WGS84) datum, zone 30 N was assigned to all datasets.

Google Earth (GE) imagery was used to collect training datasets for executing supervised classification in conjunction with CART. The Landsat imagery was classified into four LULC classes; developed, vegetation, wetlands, and water (Table 2). First, LULC polygons for each class were delineated, then 300 points were extracted by means of random sampling (1200 points total). In the study, 80% of training data collected were used to train the model while 20% of the data were used to test the model. The selection of acceptable training sites was aided by multitemporal Google Earth imagery, world street maps, and the researchers' expertise in the study area. The selected model training and LULC classification data followed a uniform distribution across the study area; equal numbers of training points in each class were sampled across the study area. Existing Google Earth images corresponding to the 2002 study area had a lower resolution compared to recent years (2013 and 2020). This is especially noticeable when trying to pinpoint areas related to small city patches or inland waters. Therefore, multi-year NDVI, MNDWI, and NDBI datasets were created along with the preprocessed bands to support the generation of training data. The methodological workflow for the study is shown in Figure 2.

Collection of Spatial Variables

Numerous biophysical, social-economic, proximate, and political factors influence LULC changes. For example, biophysical factors such as topography and climate have been shown to have a significant impact on human activities (Addae & Oppelt, 2019; Kamaraj & Rangarajan, 2022). In addition, social-economic factors, such as population, GDP, and proximate factors, such as distance from roads, towns, or rivers, are likely to affect changes in landscape patterns (Hakim et al., 2019; Bhandari et al., 2021). Development of infrastructure may be connected with urban increase and additionally results in LULC conversion, particularly in Latin America, Asia, and Africa. Other factors, including political issues such as war and policy, are influencing changes in LULC. This study used biophysical and proximate factors to model LULC change.

Correlation coefficients such as Pearson's *r* and Crammer's V are used to test the strength of relationships between driver variables and LULC changes. Assessing the correlation before modeling the transition potential is essential, as computational performance can be significantly improved when highly correlated explanatory variables are excluded. A Pearson's *r* is a number between -1 and +1 where the value of -1 indicates a full negative linear correlation, 0 being no correlation, and + 1 meaning a full positive correlation. Crammer's V ranges from 0.0 to 1.0, with a value of 1.0 indicative of a very strong association and a value approaching 0.0 indicating little or no correlation between the driver variable and land use changes. Values are not considered definitive and values above 0.1 are usually considered useful.

LULC Classification and Accuracy

Land cover classification using DT methods is more convenient and efficient (Otukei & Blaschke, 2010; Wang et al., 2014; Yang et al., 2017). In a decision tree, each stage is based on a hierarchical decision scheme or tree-like architecture. Trees contain a root node that contains all data, a variety of internal nodes, and a set of terminal nodes (leaves). The decision tree's nodes make binary decisions that separate one or more classes from the remaining classes. In general, processing occurs when moving down the tree until a leaf node is reached. The basic concept of a decision tree is to simplify a complex decision into several simpler ones, which leads to a simplified solution. This technique was used to assign each pixel to one of several classes based on its spectral sensitivity. Because the development of a decision tree necessitates supervised training, a training dataset including independent and dependent variables is required (Figure 3). The decision tree was built using R (https://cran.r-project.org) programming software and includes independent and dependent variables.

The classification results were evaluated based on a confusion matrix, using four validation metrics including Cohen's kappa coefficient (k), overall accuracy (OA), producer's accuracy (PA), and user's accuracy (UA). The Cohen's kappa is a measure of agreement standardized on a scale of -1 to 1. Values above 0.6 are considered high agreement whereas values that are less than 0.4 or negative indicate discordance (Zec et al., 2017; Alam et al., 2021; Devi et al., 2022; Kamaraj & Rangarajan, 2022). The producer accuracy tells us whether or not a sample is likely to be correctly classified whereas the user accuracy shows the likelihood that a sample from the classified map is representative of that category on the ground (Story, 1986; Halmy et al., 2015). For each class, the producer and user accuracy were computed, as well as the overall accuracy for the classes. The kappa (k) coefficient is calculated by (Kamaraj & Rangarajan, 2022):

$$k = \frac{Po - Pe}{1 - Pe}$$

where Po is the proportion of observations in agreement, Pe is the proportion of expected agreement.

The post-classification change detection method was used to quantify, identify, and analyze the discrepancies in the produced land-use maps. Using the classified images, this technique is able to generate a complex change matrix while also limiting the impacts of sensor and atmospheric changes (Singh, 1989; Addae & Oppelt, 2019). The rate of LULC change was assessed by the dynamic degree (*DD*) modeling approach. The *DD* of a single land use type indicates the rate of land use change of that particular use type within a certain time range. Based on the following equation (Nath et al., 2020), the *DD* can be computed:

$$DD = \frac{Ay - Ax}{Ax \times T} \times 100\%$$

where *Ax* is the area in the initial year, *Ay* is the area in the final year, and *T* is the temporal scale (i.e., the length of the study period). In this study, *T* represented the years between the time periods.

Methodological Approach

This study required a model that predicted the state of wetlands in GAMA in the years 2030 and 2040, so it was calibrated and validated by simulating LULC in 2020. In order to determine this, the spatio-temporal changes in the LULC classes, as well as the transition probabilities between study intervals (2002 – 2013), were derived. LULC types that underwent a transformation as well as those that remained unaltered are revealed in the change maps. The transition potential was developed using a set of driver variables that represented the key influences on change in the region. The LULC data and explanatory variables were used to derive a transition probability matrix, with rows and columns of landscape categories in the initial and final years. The transition potential model in this study was derived using the ANN multi-layer perception method. An analysis of spatial patterns and a literature review of similar studies were used to select the variables. Elevation, slope, distance from towns, distance from rivers, and distance from roads were the driver variables used in this study (Figure 4).

Distance drivers are representative of the proximity of pixels to forces that act as constraints to change. Distance from road drivers gave an indication of pixels' accessibility to roads in the region. Elevation and slope also helped to determine the geophysical limitations in the region. Physical and anthropogenic impacts on LULC dynamics can be measured with these variables as part of LULC change analysis. In this study, drivers were reclassified on a scale of 1-5 based on their proximity or value. The areas with the least distance in the study area would be in class 1 whereas the areas with the farthest distance are in class 5. These thresholds were determined by equal distances. For instance, the pixels that are within one kilometer of a major road will be shown in class 1, whereas pixels within two kilometers of a major road will be shown in class 2. A sensitivity analysis was conducted to determine which driver played the most important role in the modeling process by comparing the accuracy derived from different scenarios while altering combinations of different drivers. The integrated open-source CA-ANN multi-temporal approach followed, using the Modules for Land Use Change Simulations (MOLUSCE) plugin in Quantum GIS (QGIS).

The CA provides the spatio-temporal framework for LULC, whereas the ANN governs the local transition rules which are updated with each new time-step based on the local evolution rules. The LULC for 2020 was predicted using LULC data from 2002 and 2013, explanatory variables, and a transition matrix. The kappa validation technique was used as a comparison of actual and predicted LULC images to validate the model and prediction accuracy (Figure 5). Validation was performed to assess the CA-ANN model's ability to predict LULC for the years 2030 and 2040 in the study area. To project the LULC for 2020, 200 iterations and a neighborhood value of 3 x 3 pixels, a learning rate of 0.001, 5 hidden layers, and 0.001 momentum were chosen in the ANN learning process (Figure 6).

Land-use change models based on CA often emphasize neighborhood interactions as one of the primary driving factors (Verburg et al., 2004). Li & Li (2015) investigated the effects of neighborhood size on model performance and revealed that as the neighborhood size increased, both the overall accuracy and kappa coefficients increased slightly. The increase, however, was not significant enough to affect the results. Again, the learning rate affects how quickly network weights are tuned to learn the characteristics of input data. At a small learning rate, minor adjustments to the weights are applied and the learning process is very slow, resulting in slow convergence. Conversely, if the rate of learning is too high, the network is unusable because the weights oscillate. By incorporating the momentum factor, one can control the weight oscillation and avoid problems when searching for a minimum value on the error surface. The momentum factor may also be used to speed up the convergence process (Gorsevski et al., 2016). In this project, LULC data from 2013 and 2020 was used to forecast the LULC in 2030 and 2040 after receiving satisfactory results from model validation.

RESULTS AND DISCUSSION

Figure 7 shows the land use maps generated by CART for the years (a) 2002, (b) 2013, and (c) 2020. For example, the maps in Figures 7(a) and 7(b) were classified using Figure 3. In comparison with vegetation and wetland classes, water and development were depicted by simpler rules. Water was depicted using SWIR exceeding a particular threshold, 17.5 for CART 2002 and 29.5 for CART 2013. In CART 2002 and 2013, developed was depicted at the first internal node by RED greater than 47.5 and 51.5, respectively. The MNDWI was used to depict vegetation and wetland that had more complex rules after going through several nodes.

As Figure 7(d) shows, the developed class dominates the landscape of the study area, approximately 55% of the total area while wetlands had the lowest class percentage (less than 8%) and vegetation coverage tended to decline the most from 2002 to 2020. For the 20% of remaining training data (60 grid cells per class) used for validation, the average user and producer accuracy was above 90% for each class. The overall accuracy exceeded 90% and kappa indices of agreement exceeded 0.8 (Table 3). It was apparent that there was some confusion between some LULC classes, which showed lower user and producer accuracies of 79-89% (Table 4). In 2002 and 2013, the wetlands LULC class was easily confused with vegetation because images used in the analysis were acquired during the dry season when moisture content may be reduced or non-existent, thus causing these areas to be classified as vegetation due to the dominant reflectance of hydrophytes.

In order to determine historical changes in LULC, Landsat images from 2002, 2013, and 2020 were analyzed on a temporal basis at equal intervals. Cloud-free months were considered in this study to maintain similarity in inter-cluster and intra-cluster variability. As seasonal changes are always reflected in the image for classes such as vegetation or water, it is best to use images from a particular season to understand how the classes have changed. It would have been more appropriate to consider the 2011 images instead of 2013 in this study if strict equal intervals were to be maintained. Consequently, in this study, Landsat images from 2013 were used instead of 2011 in order to maintain image clarity and quality could be maintained. It was impossible to obtain cloud-free and noise-free Landsat images for the study area in 2011. Similarly, the model calibration was based on 2013 Landsat imagery rather than 2011 data with the assumption that no significant change had occurred between these two years. Thus, in order to generate change scenarios for 2020, the LULC map of 2002 and 2013 were analyzed, whereas 2020 data was used for the validation of the model.

LULC classes were analyzed using a change detection analysis from 2002 to 2020. The *DD* is the annual rate of change in each LULC class. For the four LULC classes, the annual change rates are found to be 1.88%, -2.47%, 1.63%, and 0.06%, for developed, vegetation, wetland, and water, respectively (Table 5). Positive annual change rates indicate an area's growth rate over time. In the period being investigated, the increase is evident from 2002-2020. Alternatively, negative change indicates the rate at which an area decreases. An annual change rate of -2.47% for vegetation, for instance, indicates that vegetation area is declining at a rate of 2.47%. Nonetheless, as can be seen from Figure 8, the percentage of transformation computed by the *DD* is inconsistent between 2002 and 2013, as well as 2013 and 2020.

During the period 2002-2013, wetlands decreased by 0.31 % annually, while they increased by 4.8 % yearly from 2013 to 2020. The waterbodies class increased by 0.19 % annually from 2002 to 2013 but decreased by 0.13 % from 2013 to 2020. Vegetation declined continuously in different periods at different rates, such as 3.33 % from 2002 to 2013 and 1.78 % between 2013-2020. An increasing trend rate was observed in the Developed class, such as a soaring 2.85 % in 2002-2013, and a slowly increasing 0.27 % in 2013-2020. Rapid urbanization is driving the decline of vegetation and other classes, as shown by the increase in the rate of change for developed classes. Several researchers have made similar observations (Akubia & Bruns, 2019; Ashiagbor et al., 2019; Nath et al., 2020).

For each phase, the areal coverage gains or loss, as depicted in Figure 8, indicates an increase in developed class and a reduction in natural areas, such as vegetation cover. During certain time intervals, however, certain classes of land cover revealed atypical behavior. While wetlands were the least notable land type for each LULC period (less than 6% coverage of the entire study area), they showed an increase of nearly 5% from 2013 to 2020. Floods in the region have been exacerbated by climatic changes over the past decade, which may explain the changes in wetland class rates. According to Intergovernmental Panel on Climate Change (IPCC) forecasts, the average monthly precipitation in Accra has increased from 160 mm in 1991-2010 to 200 mm in 2011-2020 (Asumadu-Sarkodie et al., 2015).

Transitional Potentials in the LULC Dynamics

Table 6 shows the transition probability matrix for 2002–2013, with vegetation and wetlands more likely to become developed land cover with probabilities of 0.42 and 0.17 respectively. Based on this same period, there is a 0.4 probability that wetlands will be turned into vegetation. In some cases, this may be influenced by the proximity of wetlands to towns, where wetlands are often converted into vegetable gardens for food. The LULC transition between two same classes (wetland to wetland, developed to developed) indicates that the class is likely to persist for the time interval. For instance, for the period 2002-2013, the likelihood of developed and waterbodies remaining the same is 0.93 and 0.99, respectively, which means that 93% and 99% of the area would remain unchanged (Table 6). Similarly, the transition probability between two classes over a specific time period indicates the likelihood of moving from one class to another. The transition probability of 0.42 between vegetation and developed land between 2002 and 2013 indicates that there is a 42 % of chance for the vegetation land cover to transition to developed area by 2013. According to the study, the chances of vegetation and wetland cover converting to developed land cover have been calculated to be 0.46 and 0.27, respectively, for the period 2002-2020 (Table 7). In terms of transition probability values, vegetation lands are highly susceptible to becoming developed lands. Furthermore, waterbodies and developed land cover were persistent throughout both time periods. For instance, the probability of water converting to another land cover is less than 0.007 at any point in time.

Table 8 discusses the maximum kappa coefficients and overall accuracy for various spatial combinations. The analysis concluded that all variables were good predictors of the LULC map, with all different combinations exhibiting a kappa value greater than 0.6. From the sensitivity analysis, the combination without elevation showed the highest kappa and percentage of correctness indicating the least influence from elevation considering all the other variables. Moreover, the analysis highlights distance from rivers and distance from roads as the most influential factors.

LULC Prediction and Validation

An analysis of the areal statistics for each class of LULC features comparing observed and simulated data for the year 2020 can be found in Figure 9. A comparison of the results also indicates that the model over-predicts waterbodies and developed land types, whereas it underpredicts wetlands and vegetation. The simulated and observed LULC maps of 2020 were compared (Figure 10). The overall simulation success of the CA-ANN model is 78.50 % and the current kappa value is 0.70, which has been considered satisfactory (Table 8).

Figure 11 shows the predictive output, along with the spatial distribution of these potential future scenarios of LULC. Table 9 offers a statistical analysis of the future predictions. During the period 2020–2040, the area of developed land is predicted to increase significantly, along with a loss of vegetation and wetlands. Furthermore, developed lands spread outward in a west-east direction and towards the north of the study area in agreement with observations from other studies (Osei et al., 2013; Stemn & Agyapong, 2014). For instance, towns on the outskirts of GAMA, Pokuase and Oyarifa, as well as their immediate neighboring towns (those adjacent to the Eastern region of Ghana, which borders Greater Accra region at the north), are expected to grow rapidly in terms of developed land. In contrast to the rapid growth of developed areas during the entire study period, there was little growth in areas of high elevation and slope (north-northwest of GAMA). Deforestation was especially prone to occur in vegetation adjacent to developed areas and existing in small patches. According to the study, the main road network that passes through the region is responsible for the growth of developed areas in the study area. The analysis of all predicted results shows the need for better protection of the environment and preservation of natural land cover in the study area is important, considering there are two Ramsar sites in the region that are of international significance.

Figure 12 shows the future LULC rate of change (gains/losses) in each class over different time periods. The annual growth rate of developed land cover was predicted to be 1.20% between 2020 and 2030, and 0.32% between 2030 and 2040. Urbanization was expected to be most intense from 2020 to 2030. The model also predicts that developed land cover will grow at an average annual rate of 0.86 % over the period 2002-2040 (Table 9). There is a significant declinature in vegetation land predicted in the next few decades, with an average annual rate of 3.92 % between 2020 and 2030 and 2.27 % between 2030 and 2040. For wetland cover, the model predicts an annual decline rate of 3.10% and a remarkable annual growth rate of 2.02% for the time intervals 2020-2030 and 2030-2040, respectively. In each future scenario, the amount of water bodies is predicted to change by less than 0.05% annually (Figure 12 and Table 9).

The derived LULC maps were also used to find the proportions of pervious and impervious surface areas (Figure 13). Pervious and impervious describe the ability of water to penetrate the earth's surface. Thus, pervious areas allow easy penetration of water whereas impervious regions allow little to no water penetration. Consequently, impervious areas allow more surface runoff, which promotes flooding. Generally, the developed class was assumed to be impervious since it is dominated by roads, concrete structures, and pavements, whereas other classes (vegetation, wetland, water) were assumed pervious. According to the study, the impervious to pervious surface ratio has been increasing over the last two decades (2002-2020). The percentage of pervious land was 59% in 2002, while 41% of the land was impervious. The proportion of impervious areas increased to around 54% in the recent scenario for 2020. The predicted results for 2040 climbed to 64% for impervious surfaces and a reduction of 36% for pervious surfaces (Figure 13). In the study period, the impervious to pervious ratio will reach 1.76 by 2040, up from 0.68 in 2002 and 1.19 in 2020. A significant decrease in the pervious surface is predicted during the next decade (2020-2030) based on the analysis. Urbanization and other human activities have greatly impacted all LULC classes from 2020 to 2040, including vegetation, wetlands, and water bodies. Based on the LULC map of 2040, the pervious surface area has been significantly reduced, which could indicate a potentially hazardous environment in the future. It is evident that landscape maintenance and development are needed given the destruction of natural land cover.

An increase in developed land cover is attributed to increased population growth and associated housing production, as well as non-residential built-up development, for example, industrial and commercial areas. Humans utilize the land in numerous ways and for a variety of purposes, among all natural resources (Devi et al., 2022). In this way, the LULC pattern of a region is directly influenced by population change (Owusu, 2012; Akubia & Bruns, 2019; Addae & Oppelt, 2019; Ashiagbor et al., 2019; Ekumah et al., 2020; Alam et al., 2021).

With specific reference to GAMA, its population increased by more than 50% between 1984 and 2014, with an annual growth rate of 4% (Ashiagbor et al., 2019). In addition to its long history as a trading hub, Accra's diverse economy (i.e., manufacturing, services, trade, and construction) and its high property values attract many domestic and international migrants leading to significant LULC change within its boundaries. As Songsore, (2010) noted, the high urbanization of Accra is attributed to the city being the main destination of rural-urban migration in Ghana. Its status as the largest and most developed city in Ghana has made Accra the destination of choice for many migrants because it provides them with good job opportunities, social amenities, and relative peace and stability.

This LULC study has provided evidence of rapid urbanization in GAMA and a perspective on the region's future. It contains valuable information on where urban expansion is likely to occur in the upcoming years to land planning and management officials. The stakeholders in GAMA’s urban development can thus make informed decisions regarding neighborhood design and planning, and amenities provision, as well as policy formulation and implementation based on the projections. Efforts need to be focused on the urban fringes, where most of the urban growth will take place.

Additionally, there are also significant implications for the environment in the region from this study. The protection of GAMA's wetlands is critical because they can help to control floods in addition to its other environmental services. As GAMA's population grows, however, the remaining wetlands could be encroached upon as people compete for any available land. Further, the vegetation cover of the region is expected to dwindle due to urbanization. In addition to destroying many areas of ecological importance, the destruction of these areas will also increase the amount of flooding, and air pollution in this area unless remedial measures are taken. In particular, encroachment regulations on wetlands must be developed and enforced strictly in GAMA to protect them.

Urban planning and policy formulation should fully utilize the power of urban simulation and modeling as this study exemplified through its focus on GAMA's wetlands. An effective way to compare alternative scenarios is to consider population and economic projections and likely future space demands. A variety of future land-use models can be tested using multiple policy scenarios and perspectives which can provide a robust framework for urban planning and management and decision-making in GAMA (Pan et al., 2018; Addae & Oppelt, 2019).

However, the model study is not without limitations despite its effective simulations. For instance, the model overpredicts the values of developed land types and water bodies, while underestimating the values of vegetation and wetlands. Moreover, the simulations did not include all possible drivers of LULC change such as the density of the population, the economy, and regional government policies. With a more or better representation of drivers in the model, forecasting can be enhanced (Kale et al., 2016; Bhandari et al., 2021)

CONCLUSIONS

In this research, an integrated CA-ANN approach was used to forecast future LULC scenarios within a highly urbanized GAMA region. The integration of CART-based supervised classification of multi-temporal Landsat imagery (2002, 2013, 2020) and other socio-economic, spatial, and environmental variables (elevation, slope, distance from roads, distance from towns, distance from rivers) was used to produce potential transition maps for analyzing and modeling GAMA's LULC dynamics. The prediction of future LULC in the GAMA region was carried out by the CA-ANN model embedded in the MOLUSCE plugin of QGIS. LULC maps were generated and validated with Landsat data from 2002 to 2020 using the decision tree classification technique. A spatiotemporal analysis of LULC maps in GAMA shows the significant expansion of developed land while vegetation is decreasing. Changes in LULC have been accelerated by socio-economic development and human encroachment into the natural landscapes. Furthermore, computation of the annual growth rate, considering the dynamic degree of LULC, yielded a negative trend in vegetation at an annual rate of -2.47% per year. In the period 2002-2013, water bodies increased by 0.19 % while declining by -0.13 % between 2013 and 2020. In contrast, wetlands decreased by -0.31% annually from 2002-to 2013, before showing an increase of 4.85% per year. In all three periods, wetlands accounted for the least percentage of the area.

In the GAMA region, developed land cover is increasing at the expense of vegetation land. By using the CA-ANN model, LULC transition potentials and simulated maps were derived using classified LULC maps and the driving factors such as elevation, slope, distance from roads, distance from rivers, and distance from rivers. All of these factors played a significant role in LULC changes. While developed areas were increasing across the study area, they did not show much growth where slope and elevation were high. This model's overall accuracy is 78% and it is reliable because its kappa statistic is greater than 0.63.

After validation, the MLP-ANN algorithm is applied to simulate future transformations in 2030, and 2040. LULC maps for the corresponding years were predicted using the CA model. In the immediate future, the study area is expected to undergo rapid urbanization, resulting in a high rate of deforestation with vegetation adjacent to developed areas and those existing in small patches will be most vulnerable.

The study showed that the proportion of pervious to impervious surfaces increased from 0.68 to 1.76 between 2002 and 2040. Some of the increases in impervious surfaces are likely to come at the expense of wetlands. Land-use policies are therefore important in guiding the sustainable development of GAMA since they reduce threats to natural resources. It is therefore recommended that Ghana's national and regional governments pay immediate attention to GAMA's spatial growth. These governments should create and enforce regulations on land use change because it is the primary cause of disruptions in the environment including wetland losses. Planning for efficient land use management can be achieved by using the insights provided by this study.

Based on the simulated distribution of the LULC classes in GAMA in 2030 and 2040, the landscape will likely continue to undergo the changes observed in the recent past. These changes need to be evaluated in more detail to determine the expected impacts. It is recommended that future analyses use more detailed socio-environmental variables to better understand the causes, locations, and trends of land use changes in the region. Moreover, future studies should expand the study area in order to establish similar trends across the entire Greater Accra region.

REFERENCES

Abbas, Z., Yang, G., Zhong, Y., & Zhao, Y. (2021). Spatiotemporal Change Analysis and Future Scenario of LULC Using the CA-ANN Approach: A Case Study of the Greater Bay Area, China. *Land*, *10*(6), 584. https://doi.org/10.3390/land10060584

Abdullah, A. Y. M., Masrur, A., Adnan, M. S. G., Baky, Md. A. A., Hassan, Q. K., & Dewan, A. (2019). Spatio-temporal Patterns of Land Use/Land Cover Change in the Heterogeneous Coastal Region of Bangladesh between 1990 and 2017. *Remote Sensing*, *11*(7), 790. https://doi.org/10.3390/rs11070790

Aboelnour, M., & Engel, B. A. (2018). Application of Remote Sensing Techniques and Geographic Information Systems to Analyze Land Surface Temperature in Response to Land Use/Land Cover Change in Greater Cairo Region, Egypt. *Journal of Geographic Information System*, *10*(01), 57–88. https://doi.org/10.4236/jgis.2018.101003

Aburas, M. M., Ho, Y. M., Ramli, M. F., & Ash'aari, Z. H. (2016). The simulation and prediction of spatio-temporal urban growth trends using cellular automata models: A review. *International Journal of Applied Earth Observation and Geoinformation*, *52*, 380–389. https://doi.org/10.1016/j.jag.2016.07.007

Adade, R., Nyarko, B. K., Aheto, D. W., & Osei, K. N. (2017). Fragmentation of wetlands in the south eastern coastal savanna of Ghana. *Regional Studies in Marine Science*, *12*, 40–48. https://doi.org/10.1016/j.rsma.2017.03.003

Addae, B., & Oppelt, N. (2019). Land-Use/Land-Cover Change Analysis and Urban Growth Modelling in the Greater Accra Metropolitan Area (GAMA), Ghana. *Urban Science*, *3*(1), 26. https://doi.org/10.3390/urbansci3010026

Akubia, J. E. K., & Bruns, A. (2019). Unravelling the Frontiers of Urban Growth: Spatio-Temporal Dynamics of Land-Use Change and Urban Expansion in Greater Accra Metropolitan Area, Ghana. *Land*, *8*(9), 131. https://doi.org/10.3390/land8090131

Alam, N., Saha, S., Gupta, S., & Chakraborty, S. (2021). Prediction modelling of riverine landscape dynamics in the context of sustainable management of floodplain: A Geospatial approach. *Annals of GIS*, *27*(3), 299–314. https://doi.org/10.1080/19475683.2020.1870558

Allam, M., Bakr, N., & Elbably, W. (2019). Multi-temporal assessment of land use/land cover change in arid region based on landsat satellite imagery: Case study in Fayoum Region, Egypt. *Remote Sensing Applications: Society and Environment*, *14*, 8–19. https://doi.org/10.1016/j.rsase.2019.02.002

Arzandeh, S., & Wang, J. (2002). Texture evaluation of RADARSAT imagery for wetland mapping. *Canadian Journal of Remote Sensing*, *28*(5), 14.

Ashiagbor, G., Amoako, C., Asabere, S. B., & Quaye-Ballard, J. A. (2019). Landscape Transformations in Rapidly Developing Peri-urban Areas of Accra, Ghana: Results of 30 years. *Open Geosciences*, *11*(1), 172–182. https://doi.org/10.1515/geo-2019-0014

Asumadu-Sarkodie, S., Owusu, P. A., & Rufangura, P. (2015). *Impact analysis of flood in Accra, Ghana*. 26.

Awotwi, A., Anornu, G. K., Quaye-Ballard, J. A., Annor, T., Forkuo, E. K., Harris, E., Agyekum, J., & Terlabie, J. L. (2019). Water balance responses to land-use/land-cover changes in the Pra River Basin of Ghana, 1986–2025. *Catena*, *182*, 104129. https://doi.org/10.1016/j.catena.2019.104129

Balogun, I. A., & Ishola, K. A. (2017). Projection of Future Changes in Landuse/Landcover Using Cellular Automata/Markov Model over Akure City, Nigeria. *Journal of Remote Sensing Technology*, *5*(1), 22–31. https://doi.org/10.18005/JRST0501003

Bhandari, S., Twayana, R., Shrestha, R., & Sharma, K. (2021). *Future Land Use Land Cover Scenario Simulation Using Open-Source GIS for the City of Banepa and Dhulikhel Municipality, Nepal*.

Christovam, L. E., Pessoa, G. G., Shimabukuro, M. H., & Galo, M. L. B. T. (2019). Land use and land cover classification using hyperspectral imagery: Evaluating the performance of spectral angle mapper, support vector machine and random forest. *The International Archives of the Photogrammetry, Remote Sensing and Spatial Information Sciences*, *XLII-2/W13*, 1841–1847. https://doi.org/10.5194/isprs-archives-XLII-2-W13-1841-2019

Devi, A. B., Deka, D., Aneesh, T. D., Srinivas, R., & Nair, A. M. (2022). Predictive modelling of land use land cover dynamics for a tropical coastal urban city in Kerala, India. *Arabian Journal of Geosciences*, *15*(5), 399. https://doi.org/10.1007/s12517-022-09735-7

Dronova, I. (2015). Object-Based Image Analysis in Wetland Research: A Review. *Remote Sensing*, *7*(5), 6380–6413. https://doi.org/10.3390/rs70506380

Ekumah, B., Armah, F. A., Afrifa, E. K. A., Aheto, D. W., Odoi, J. O., & Afitiri, A.-R. (2020a). Assessing land use and land cover change in coastal urban wetlands of international importance in Ghana using Intensity Analysis. *Wetlands Ecology and Management*, *28*(2), 271–284. https://doi.org/10.1007/s11273-020-09712-5

Ekumah, B., Armah, F. A., Afrifa, E. K. A., Aheto, D. W., Odoi, J. O., & Afitiri, A.-R. (2020b). Assessing land use and land cover change in coastal urban wetlands of international importance in Ghana using Intensity Analysis. *Wetlands Ecology and Management*, *28*(2), 271–284. https://doi.org/10.1007/s11273-020-09712-5

El-Tantawi, A. M., Bao, A., Chang, C., & Liu, Y. (2019). Monitoring and predicting land use/cover changes in the Aksu-Tarim River Basin, Xinjiang-China (1990–2030). *Environmental Monitoring and Assessment*, *191*(8), 480. https://doi.org/10.1007/s10661-019-7478-0

Faisal, A., & Khan, H. A. H. (2017). Application of GIS and remote sensing in disaster management: A critical review of flood management; *Proceedings of International Conference on Disaster Risk Mitigation; Dhaka, Bangladesh.*, 23–24.

Gabrielsen, C. G., Murphy, M. A., & Evans, J. S. (2016). Using a multiscale, probabilistic approach to identify spatial-temporal wetland gradients. *Remote Sensing of Environment*, *184*, 522–538. https://doi.org/10.1016/j.rse.2016.07.034

Gallant, A. (2015). The Challenges of Remote Monitoring of Wetlands. *Remote Sensing*, *7*(8), 10938–10950. https://doi.org/10.3390/rs70810938

Ghana Statistical Service. (2010). *2010 Population and Housing Census Summary Report of Final Results; Ghana Statistical Service: Accra, Ghana*.

Gharaibeh, A., Shaamala, A., Obeidat, R., & Al-Kofahi, S. (2020). Improving land-use change modeling by integrating ANN with Cellular Automata-Markov Chain model. *Heliyon, 6(9), E05092.*

Gorsevski, P. V., Brown, M. K., Panter, K., Onasch, C. M., Simic, A., & Snyder, J. (2016). Landslide detection and susceptibility mapping using LiDAR and an artificial neural network approach: A case study in the Cuyahoga Valley National Park, Ohio. *Landslides*, *13*(3), 467–484. https://doi.org/10.1007/s10346-015-0587-0

Gosselin, G., Touzi, R., & Cavayas, F. (2014). *Polarimetric Radarsat-2 wetland classification using the Touzi decomposition: Case of the Lac Saint-Pierre Ramsar wetland*. *36*(6), 17.

Guan, D., Li, H., Inohae, T., Su, W., Nagaie, T., & Hokao, K. (2011). Modeling urban land use change by the integration of cellular automaton and Markov model. *Ecological Modelling*, *222*(20–22), 3761–3772. https://doi.org/10.1016/j.ecolmodel.2011.09.009

Guan, Q., Wang, L., & Clarke, K. C. (2005). An Artificial-Neural-Network-based, Constrained CA Model for Simulating Urban Growth. *Cartography and Geographic Information Science*, *32*(4), 369–380. https://doi.org/10.1559/152304005775194746

Hakim, A. M. Y., Baja, S., Rampisela, D. A., & Arif, S. (2019). Spatial dynamic prediction of landuse / landcover change (case study: Tamalanrea sub-district, makassar city). *IOP Conference Series: Earth and Environmental Science*, *280*(1), 012023. https://doi.org/10.1088/1755-1315/280/1/012023

Halmy, M. W. A., Gessler, P. E., Hicke, J. A., & Salem, B. B. (2015). Land use/land cover change detection and prediction in the north-western coastal desert of Egypt using Markov-CA. *Applied Geography*, *63*, 101–112. https://doi.org/10.1016/j.apgeog.2015.06.015

Hua, L., Zhang, X., Chen, X., Yin, K., & Tang, L. (2017). A Feature-Based Approach of Decision Tree Classification to Map Time Series Urban Land Use and Land Cover with Landsat 5 TM and Landsat 8 OLI in a Coastal City, China. *ISPRS International Journal of Geo-Information*, *6*(11), 331. https://doi.org/10.3390/ijgi6110331

Jayasinghe, P., Kantakumar, L. N., Raghavan, V., & Yonezawa, G. (2021). Comparative Evaluation of Open Source Urban Simulation Models Applied to Colombo City and

Environs in Sri Lanka. *International Journal of Geoinformatics*, 49–60. https://doi.org/10.52939/ijg.v17i3.1897

Job, N., Roux, D. J., Bezuidenhout, H., & Cole, N. S. (2020). A Multi-Scale, Participatory Approach to Developing a Protected Area Wetland Inventory in South Africa. *Frontiers in Environmental Science*, *8*, 49. https://doi.org/10.3389/fenvs.2020.00049

Jokar Arsanjani, J., Helbich, M., Kainz, W., & Darvishi Boloorani, A. (2013). Integration of logistic regression, Markov chain and cellular automata models to simulate urban expansion. *International Journal of Applied Earth Observation and Geoinformation*, *21*, 265–275. https://doi.org/10.1016/j.jag.2011.12.014

Kafy, A.-A., Naim, M. N. H., Subramanyam, G., Ahmed, N. U., Al Rakib, A., Kona, M. A., & Sattar, G. S. (2021). Cellular Automata approach in dynamic modelling of land cover changes using RapidEye images in Dhaka, Bangladesh. *Environmental Challenges, 4, 100084*.

Kafy, A.-A., Rahman, Md. S., Faisal, A.-A.-, Hasan, M. M., & Islam, M. (2020). Modelling future land use land cover changes and their impacts on land surface temperatures in Rajshahi, Bangladesh. *Remote Sensing Applications: Society and Environment*, *18*, 100314. https://doi.org/10.1016/j.rsase.2020.100314

Kale, M. P., Chavan, M., Pardeshi, S., Joshi, C., Verma, P. A., Roy, P. S., Srivastav, S. K., Srivastava, V. K., Jha, A. K., Chaudhari, S., Giri, Y., & Krishna Murthy, Y. V. N. (2016). Land-use and land-cover change in Western Ghats of India. *Environmental Monitoring and Assessment*, *188*(7), 387. https://doi.org/10.1007/s10661-016-5369-1

Kamaraj, M., & Rangarajan, S. (2022). Predicting the future land use and land cover changes for Bhavani basin, Tamil Nadu, India, using QGIS MOLUSCE plugin. *Environmental Science and Pollution Research*. https://doi.org/10.1007/s11356-021-17904-6

Knight, R. L., Clarke, R. A., & Bastian, R. K. (2001). Surface flow (SF) treatment wetlands as a habitat for wildlife and humans. *Water Science and Technology*, *44*(11–12), 27–37. https://doi.org/10.2166/wst.2001.0806

Kourosh Niya, A., Huang, J., Kazemzadeh-Zow, A., Karimi, H., Keshtkar, H., & Naimi, B. (2020). Comparison of three hybrid models to simulate land use changes: A case study in Qeshm Island, Iran. *Environmental Monitoring and Assessment*, *192*(5), 302. https://doi.org/10.1007/s10661-020-08274-6

Kumar, L., & Sinha, P. (2014). Mapping salt-marsh land-cover vegetation using high-spatial and hyperspectral satellite data to assist wetland inventory. *GIScience & Remote Sensing*, *51*(5), 483–497. https://doi.org/10.1080/15481603.2014.947838

Lehner, B., & Döll, P. (2004). Development and validation of a global database of lakes, reservoirs and wetlands. *Journal of Hydrology*, *296*(1–4), 1–22. https://doi.org/10.1016/j.jhydrol.2004.03.028

Li, J., & Chen, W. (2005). A rule-based method for mapping Canada's wetlands using optical, radar and DEM data. *International Journal of Remote Sensing*, *26*(22), 5051–5069. https://doi.org/10.1080/01431160500166516

Li, T., & Li, W. (2015). Multiple land use change simulation with Monte Carlo approach and CA-ANN model, a case study in Shenzhen, China. *Environmental Systems Research*, *4*(1), 1. https://doi.org/10.1186/s40068-014-0026-6

Li, X., & Yeh, A. G.-O. (2002). Neural-network-based cellular automata for simulating multiple land use changes using GIS. *International Journal of Geographical Information Science*, *16*(4), 323–343. https://doi.org/10.1080/13658810210137004

Liou, Y.-A., Nguyen, A. K., & Li, M.-H. (2017). Assessing spatiotemporal eco-environmental vulnerability by Landsat data. *Ecological Indicators*, *80*, 52–65. https://doi.org/10.1016/j.ecolind.2017.04.055

Liu, X., Liang, X., Li, X., Xu, X., Ou, J., Chen, Y., Li, S., Wang, S., & Pei, F. (2017). A future land use simulation model (FLUS) for simulating multiple land use scenarios by coupling human and natural effects. *Landscape and Urban Planning*, *168*, 94–116. https://doi.org/10.1016/j.landurbplan.2017.09.019

Losiri, C., Nagai, M., Ninsawat, S., & Shrestha, R. (2016). Modeling Urban Expansion in Bangkok Metropolitan Region Using Demographic–Economic Data through Cellular Automata-Markov Chain and Multi-Layer Perceptron-Markov Chain Models. *Sustainability*, *8*(7), 686. https://doi.org/10.3390/su8070686

Mackenzie, W., & Moran, J. (2004). *Wetlands of British Columbia: A guide to identification. Victoria, British Columbia, Research Branch, British Columbia Ministry of Forests*. *BC Land Manage Handb. 52*.

Mahdavi, Salehi, B., Granger, J., Amani, M., Brisco, B., & Huang, W. (2018). Remote sensing for wetland classification: A comprehensive review. *GIScience & Remote Sensing*, *55*(5), 623–658. https://doi.org/10.1080/15481603.2017.1419602

Mahdianpari, M., Salehi, B., Mohammadimanesh, F., & Motagh, M. (2017). Random forest wetland classification using ALOS-2 L-band, RADARSAT-2 C-band, and TerraSAR-X imagery. *ISPRS Journal of Photogrammetry and Remote Sensing*, *130*, 13–31. https://doi.org/10.1016/j.isprsjprs.2017.05.010

Manandhar, R., Odeh, I., & Ancev, T. (2009). Improving the Accuracy of Land Use and Land Cover Classification of Landsat Data Using Post-Classification Enhancement. *Remote Sensing*, *1*(3), 330–344. https://doi.org/10.3390/rs1030330

Michetti, M., & Zampieri, M. (2014). Climate–Human–Land Interactions: A Review of Major Modelling Approaches. *Land*, *3*(3), 793–833. https://doi.org/10.3390/land3030793

Ministry of Gender, Children and Social Protection. (2014). *Child Protection Baseline Research Report*.

Ministry of Lands and Forestry. (1999). Republic of Ghana. Managing Ghana's Wetlands: *A National Wetlands Conservation Strategy*.

Mitsch, W. J., Bernal, B., Nahlik, A. M., Mander, Ü., Zhang, L., Anderson, C. J., Jørgensen, S. E., & Brix, H. (2013). Wetlands, carbon, and climate change. *Landscape Ecology*, *28*(4), 583–597. https://doi.org/10.1007/s10980-012-9758-8

Mohammady, S., Delavar, M. R., & Pahlavani, P. (2014). Urban growth modeling using an artificial neural network a case study of Sanandaj city, Iran. *The International Archives of the Photogrammetry, Remote Sensing and Spatial Information Sciences*, *XL-2/W3*, 203–208. https://doi.org/10.5194/isprsarchives-XL-2-W3-203-2014

Moser, L., Schmitt, A., Wendleder, A., & Roth, A. (2016). Monitoring of the Lac Bam Wetland Extent Using Dual-Polarized X-Band SAR Data. *Remote Sensing*, *8*(4), 302. https://doi.org/10.3390/rs8040302

Nath, B., Wang, Z., Ge, Y., Islam, K., P. Singh, R., & Niu, Z. (2020). Land Use and Land Cover Change Modeling and Future Potential Landscape Risk Assessment Using Markov-CA

Model and Analytical Hierarchy Process. *ISPRS International Journal of Geo-Information*, *9*(2), 134. https://doi.org/10.3390/ijgi9020134

National Wetland Working Group. (1997). *The Canadian wetland classification system. Wetlands Research Branch, University of Waterloo*.

Niculescu, S., Boissonnat, J.-B., Lardeux, C., Roberts, D., Hanganu, J., Billey, A., Constantinescu, A., & Doroftei, M. (2020). Synergy of High-Resolution Radar and Optical Images Satellite for Identification and Mapping of Wetland Macrophytes on the Danube Delta. *Remote Sensing*, *12*(14), 2188. https://doi.org/10.3390/rs12142188

Niu, Z., Zhang, H., Wang, X., Yao, W., Zhou, D., Zhao, K., Zhao, H., Li, N., Huang, H., Li, C., Yang, J., Liu, C., Liu, S., Wang, L., Li, Z., Yang, Z., Qiao, F., Zheng, Y., Chen, Y., … Gong, P. (2012). Mapping wetland changes in China between 1978 and 2008. *Chinese Science Bulletin*, *57*(22), 2813–2823. https://doi.org/10.1007/s11434-012-5093-3

Njomaba, E., Ofori, J. N., Aikins, B. E., & Nyame, D. A. A. (2021). *Flood Risk Mapping and its Effects on livelihood in Ghana using Sentinel-1 data. A case study of Accra*. 9.

Osei, F. E., Balogun, B. O., & Afrifa, C. G. (2013). *Identifying and Quantifying Urban Sprawl in the Greater Accra Region of Ghana from 1985 to 2014*. *4*(1), 7.

Otukei, J. R., & Blaschke, T. (2010). Land cover change assessment using decision trees, support vector machines and maximum likelihood classification algorithms. *Int. J. Appl. Earth Obs. Geoinf.*, 12 S27-S31.

Owusu, G. (2012). *Coping with urban sprawl: A critical discussion of the urban containment strategy in a developing country city, Accra*.

Ozesmi, S. L., & Bauer, M. E. (2002). Satellite remote sensing of wetlands. *Wetlands Ecology and Management*, *10*(5), 381–402.

Pan, H., Deal, B., Destouni, G., Zhang, Y., & Kalantari, Z. (2018). Sociohydrology modeling for complex urban environments in support of integrated land and water resource management practices. *Land Degradation & Development*, *29*(10), 3639–3652. https://doi.org/10.1002/ldr.3106

Park, S., Jeon, S., Kim, S., & Choi, C. (2011). Prediction and comparison of urban growth by land suitability index mapping using GIS and RS in South Korea. *Landscape and Urban Planning*, *99*(2), 104–114. https://doi.org/10.1016/j.landurbplan.2010.09.001

Pattison-Williams, J. K., Pomeroy, J. W., Badiou, P., & Gabor, S. (2018). Wetlands, Flood Control and Ecosystem Services in the Smith Creek Drainage Basin: A Case Study in Saskatchewan, Canada. *Ecological Economics*, *147*, 36–47. https://doi.org/10.1016/j.ecolecon.2017.12.026

Pijanowski, B. C., Brown, D. G., Shellito, B. A., & Manik, G. A. (2002). Using neural networks and GIS to forecast land use changes: A Land Transformation Model. *Computers, Environment and Urban Systems*, *26*(6), 553–575. https://doi.org/10.1016/S0198-9715(01)00015-1

Prasad, S. V. S., Savithri, T. S., & V. Murali Krishna, I. (2017). Comparison of Accuracy Measures for RS Image Classification using SVM and ANN Classifiers. *International Journal of Electrical and Computer Engineering (IJECE)*, *7*(3), 1180. https://doi.org/10.11591/ijece.v7i3.pp1180-1187

Rendana, M., Rahim, S. A., Idris, W. M. R., Lihan, T., & Rahman, Z. A. (2015). CA-Markov for predicting land use changes in tropical catchment area: A case study in Cameron Highland, Malaysia. *Journal of Applied Sciences*, 15(4), 689-695.

Rundquist, D. C., Narumalani, S., & Narayanan, R. M. (2001). A review of wetlands remote sensing and defining new considerations. *Remote Sensing Reviews*, *20*(3), 207–226. https://doi.org/10.1080/02757250109532435

Santé, I., García, A. M., Miranda, D., & Crecente, R. (2010). Cellular automata models for the simulation of real-world urban processes: A review and analysis. *Landscape and Urban Planning*, *96*(2), 108–122. https://doi.org/10.1016/j.landurbplan.2010.03.001

Shihab, T., Al-Hameedawi, A., & Hamza, A. (2020). Random Forest (RF) and Artificial Neural Network (ANN) Algorithms for LULC Mapping. *Engineering and Technology Journal*, *38*(4A), 510–514. https://doi.org/10.30684/etj.v38i4A.399

Silva, E. A., & Clarke, K. C. (2002). Calibration of the SLEUTH urban growth model for Lisbon and Porto, Portugal. *Computers, Environment and Urban Systems*, *26*(6), 525–552. https://doi.org/10.1016/S0198-9715(01)00014-X

Singh, A. (1989). Review Article Digital change detection techniques using remotely-sensed data. *International Journal of Remote Sensing*, *10*(6), 989–1003. https://doi.org/10.1080/01431168908903939

Sobhani, P., Esmaeilzadeh, H., & Mostafavi, H. (2021). Simulation and impact assessment of future land use and land cover changes in two protected areas in Tehran, Iran. *Sustainable Cities and Society*, *75*, 103296. https://doi.org/10.1016/j.scs.2021.103296

Songsore, J. (2010). *The urban transition in Ghana: Urbanization, national development and poverty reduction*. 57.

Stemn, E., & Agyapong, E. (2014). *Assessment of Urban Expansion in the Sekondi-Takoradi Metropolis of Ghana Using Remote-Sensing and GIS Approach*. *3*(8), 10.

Story, M. (1986). Accuracy Assessment: A User's Perspective. *Photogrammetric Engineering and Remote Sensing*, 52(3), 397–399.

Sun, S., Zhang, Y., Song, Z., Chen, B., Zhang, Y., Yuan, W., Chen, C., Chen, W., Ran, X., & Wang, Y. (2020). Mapping Coastal Wetlands of the Bohai Rim at a Spatial Resolution of 10 m Using Multiple Open-Access Satellite Data and Terrain Indices. *Remote Sensing*, *12*(24), 4114. https://doi.org/10.3390/rs12244114

Tian, Y., Yin, K., Lu, D., Hua, L., Zhao, Q., & Wen, M. (2014). Examining Land Use and Land Cover Spatiotemporal Change and Driving Forces in Beijing from 1978 to 2010. *Remote Sensing*, *6*(11), 10593–10611. https://doi.org/10.3390/rs61110593

Tiner. (1999). Wetland indicators: A guide to wetland identification, delineation, classification, and mapping. *CRC Press*.

Tiner, R. W. (1991). The Concept of a Hydrophyte for Wetland Identification. *BioScience*, *41*(4), 236–247. https://doi.org/10.2307/1311413

Uuemaa, E., Hughes, A., & Tanner, C. (2018). Identifying Feasible Locations for Wetland Creation or Restoration in Catchments by Suitability Modelling Using Light Detection and Ranging (LiDAR) Digital Elevation Model (DEM). *Water*, *10*(4), 464. https://doi.org/10.3390/w10040464

Verburg, P. H., de Nijs, T. C. M., Ritsema van Eck, J., Visser, H., & de Jong, K. (2004). A method to analyse neighbourhood characteristics of land use patterns. *Computers, Environment and Urban Systems*, *28*(6), 667–690. https://doi.org/10.1016/j.compenvurbsys.2003.07.001

Wang, C., Liu, H.-Y., Zhang, Y., & Li, Y. (2014). Classification of land-cover types in muddy tidal flat wetlands using remote sensing data. *Journal of Applied Remote Sensing*, *7*(1), 073457. https://doi.org/10.1117/1.JRS.7.073457

Wu, Q., & Lane, C. R. (2017). Delineating wetland catchments and modeling hydrologic connectivity using lidar data and aerial imagery. *Hydrology and Earth System Sciences*, *21*(7), 3579–3595. https://doi.org/10.5194/hess-21-3579-2017

Yang, C., Wu, G., Ding, K., Shi, T., Li, Q., & Wang, J. (2017). Improving Land Use/Land Cover Classification by Integrating Pixel Unmixing and Decision Tree Methods. *Remote Sensing*, *9*(12), 1222. https://doi.org/10.3390/rs9121222

Yuan, T., Yiping, X., Lei, Z., & Danqing, L. (2015). Land use and cover change simulation and prediction in Hangzhou city based on CA-Markov model. *International Proceedings of Chemical. Biol. Environ. Eng*, 90(17), 108–113.

Zec, S., Soriani, N., Comoretto, R., & Baldi, I. (2017). High Agreement and High Prevalence: The Paradox of Cohen’s Kappa. *The Open Nursing Journal*, *11*(1), 211–218. https://doi.org/10.2174/1874434601711010211

Zedler, J. B., & Kercher, S. (2005). Wetland resources: Status, trends, ecosystem services, and restorability. *Annual Review of Environment and Resources*, *30*(1), 39–74. https://doi.org/10.1146/annurev.energy.30.050504.144248

APPENDIX A FIGURES

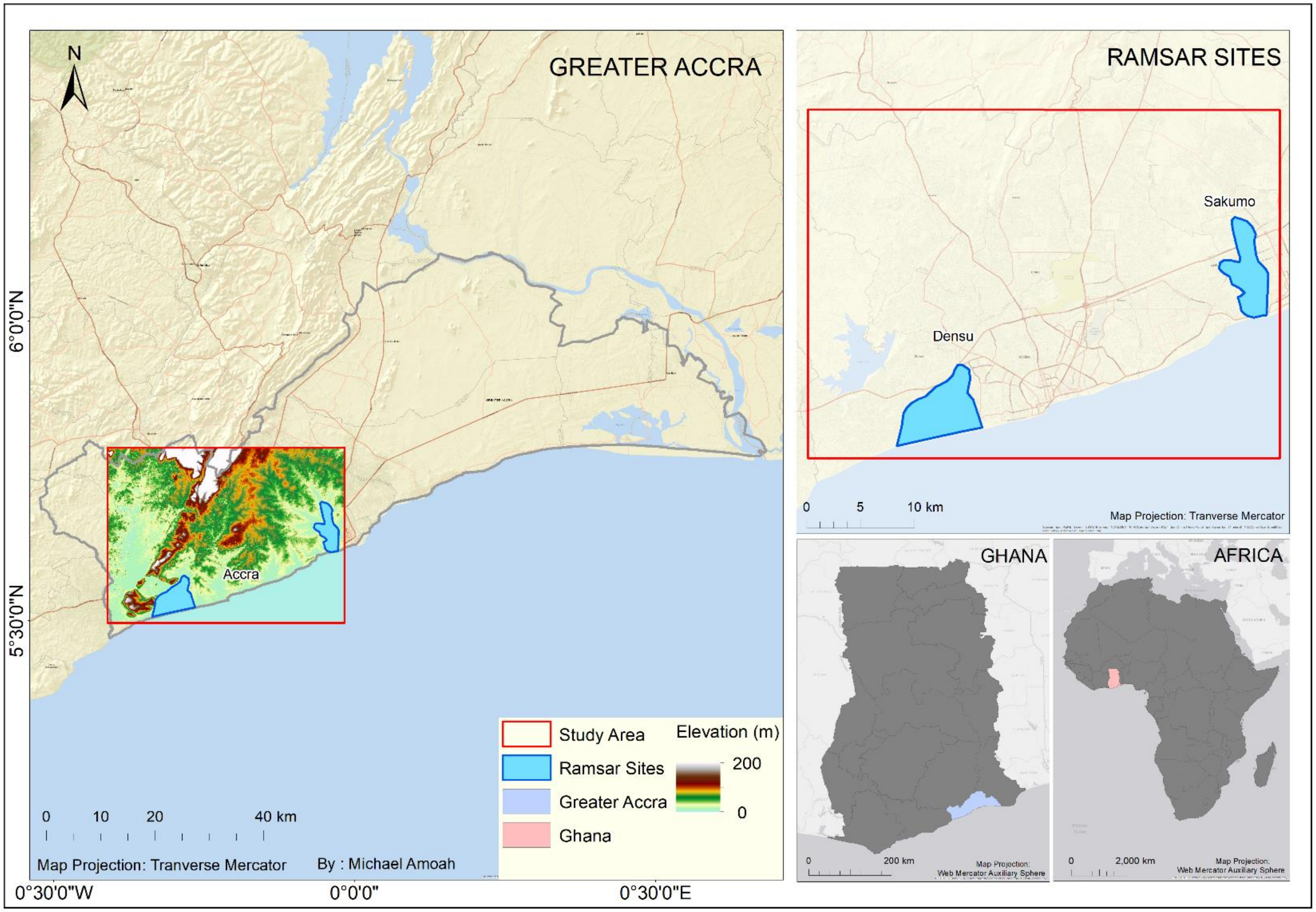

Figure 1. Location of the study area

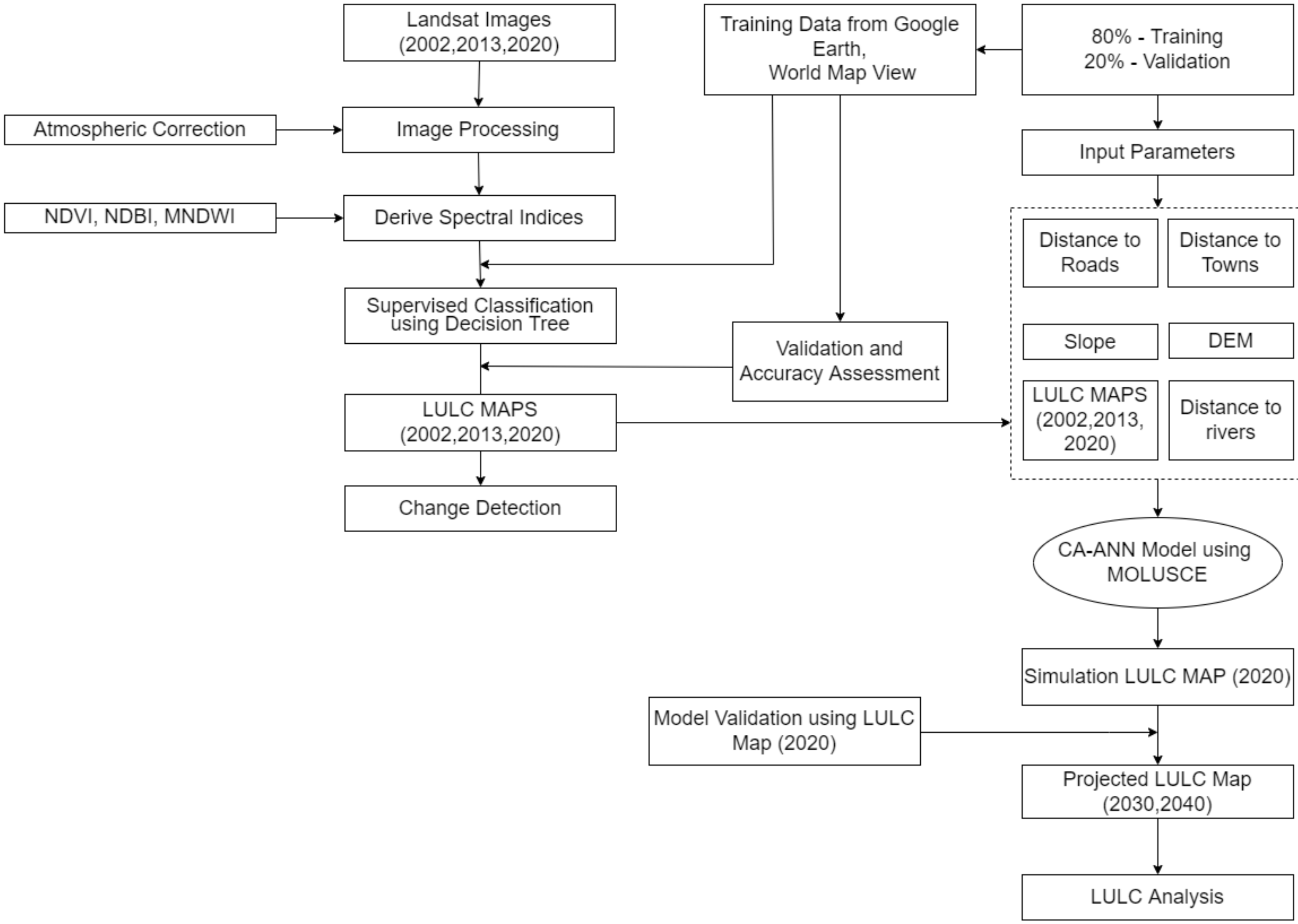

Figure 2. Flow chart of the methodology

a) *b)*

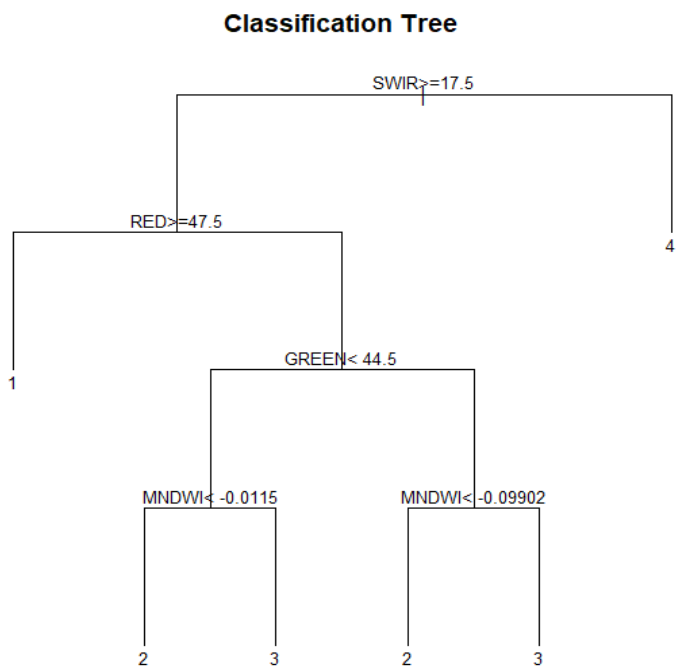

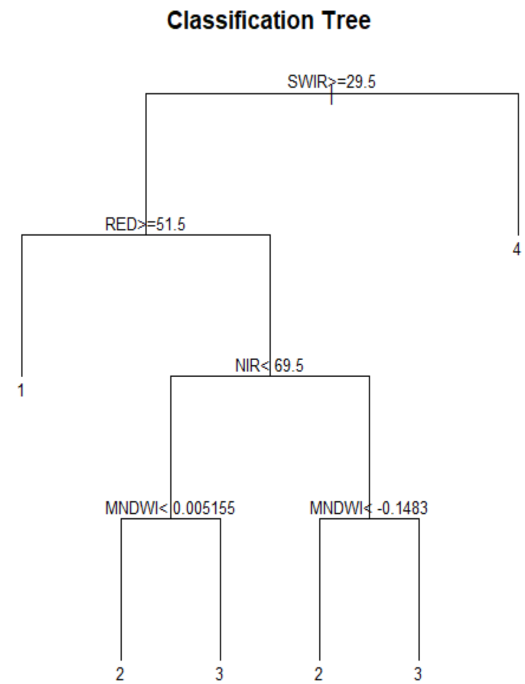

Figure 3. Diagram of CART for LULC. (a) 2002 (b) 2013 (1 - developed; 2 – vegetation; 3 – wetland; 4 – water)

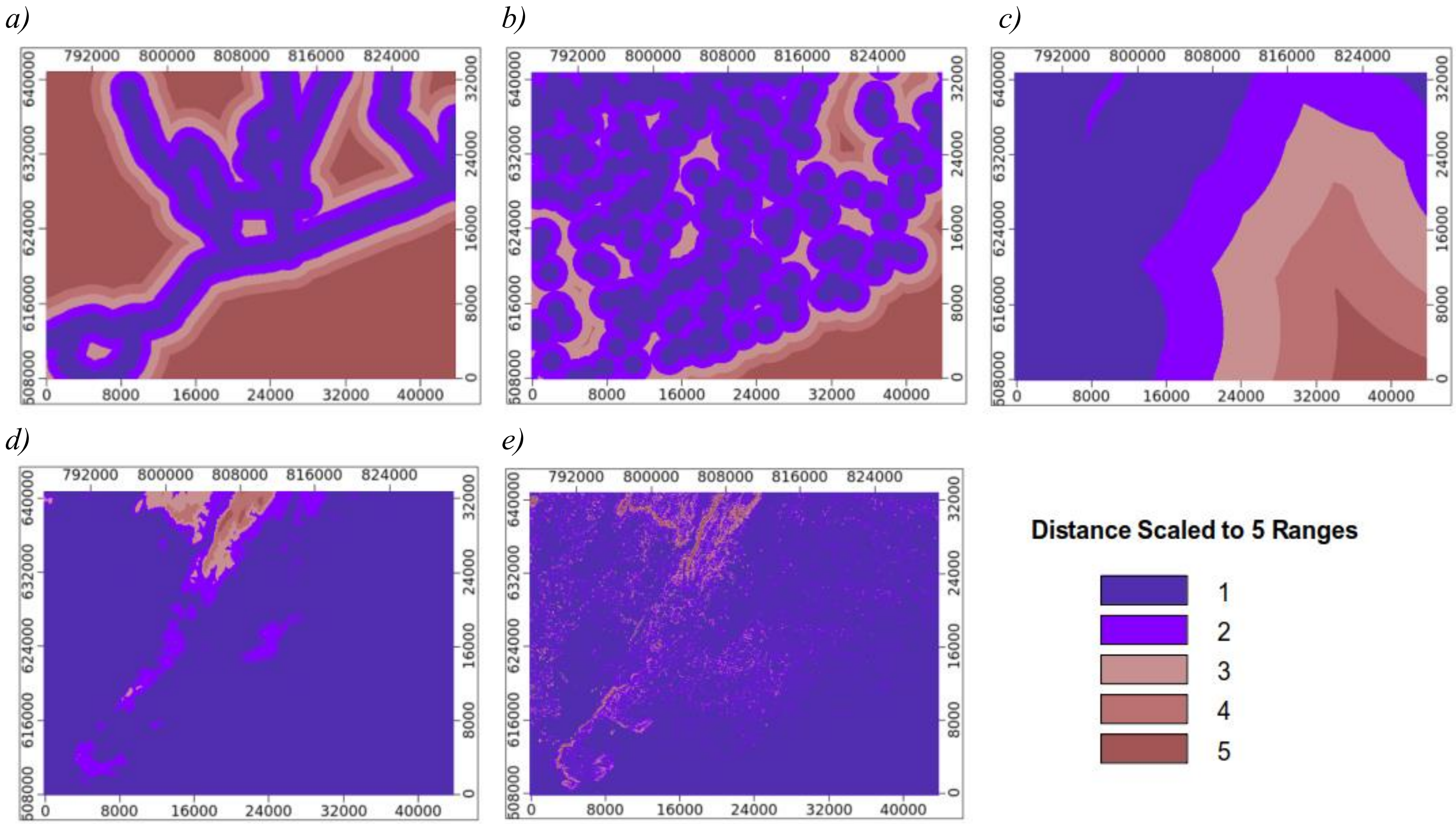

Figure 4. Spatial drivers. (a) distance from roads, (b) distance from towns, (c) distance from rivers, (d) elevation, (e) slope (thresholds were determined using equal distances such as buffered distances from roads within 1, 2, 3, 4, and greater than 5 km)

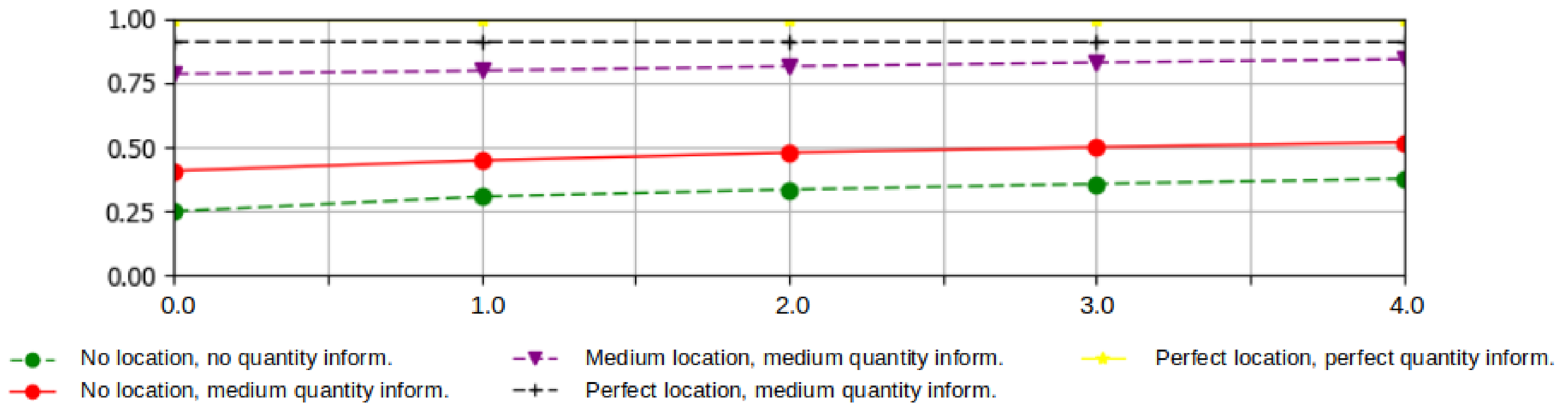

Figure 5. The validation graph between the observed 2020 LULC and predicted 2020 LULC (with kappa and maximum percentage of correctness on the y-axis and LULCs on the x-axis; 1 - developed; 2 – vegetation; 3 – wetland; 4 – water)

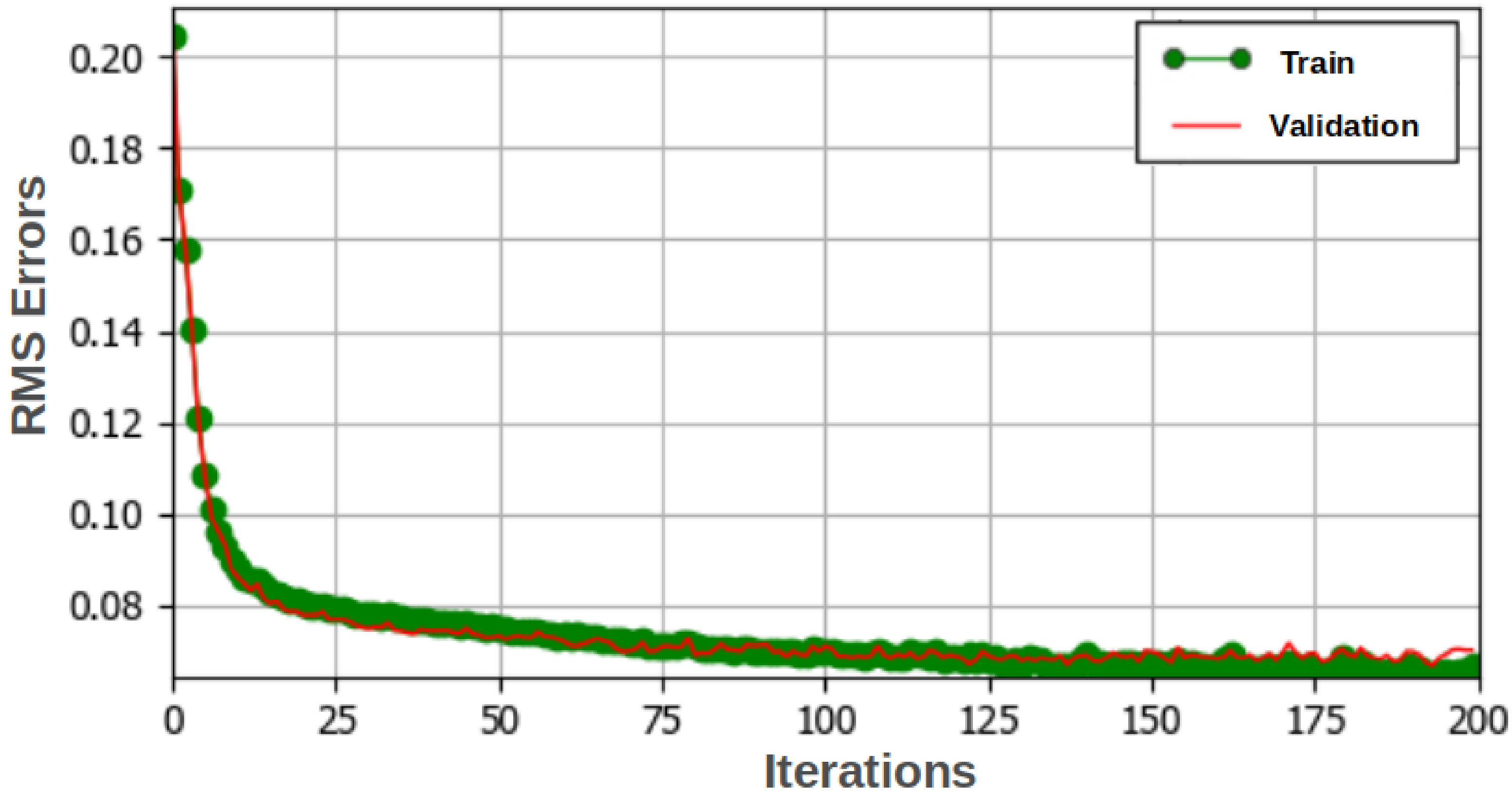

Figure 6. Neural network learning curve

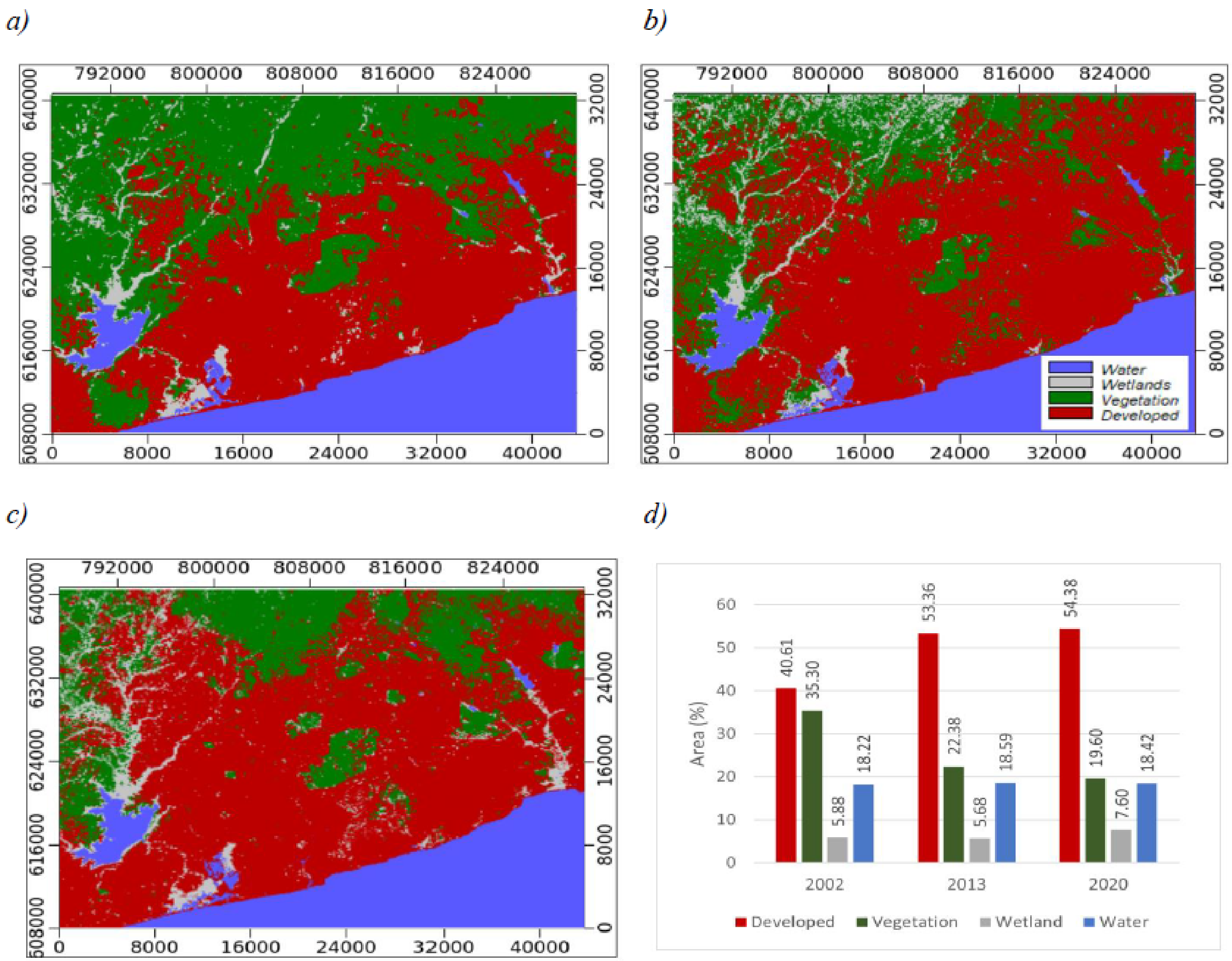

Figure 7. Distribution of LULC features in the study area. (a) Year 2002 (b) Year 2013 (c) Year 2020 and (d) LULC percentage cover.

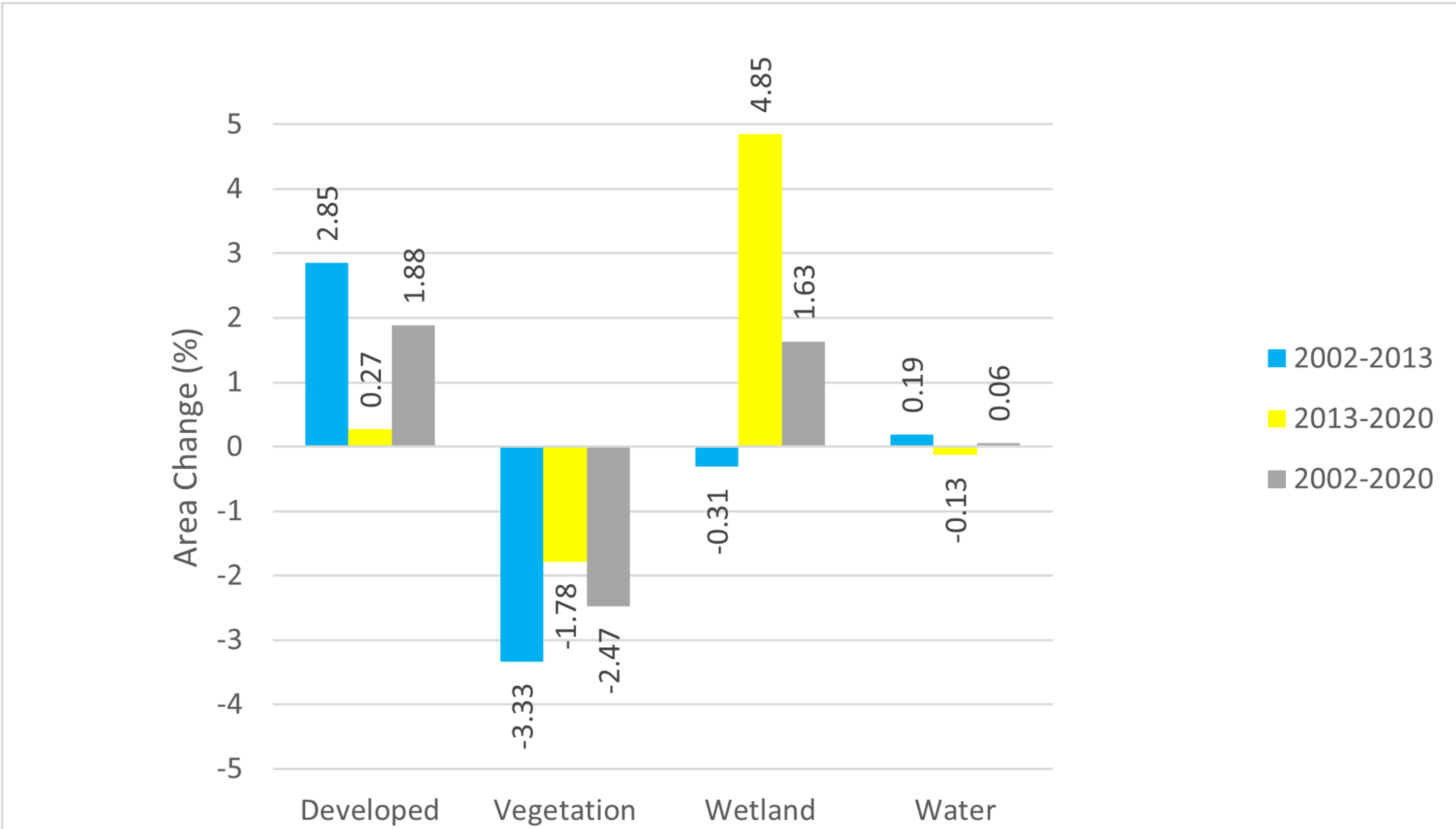

Figure 8. Area percentage change rate for LULC classes for different time periods

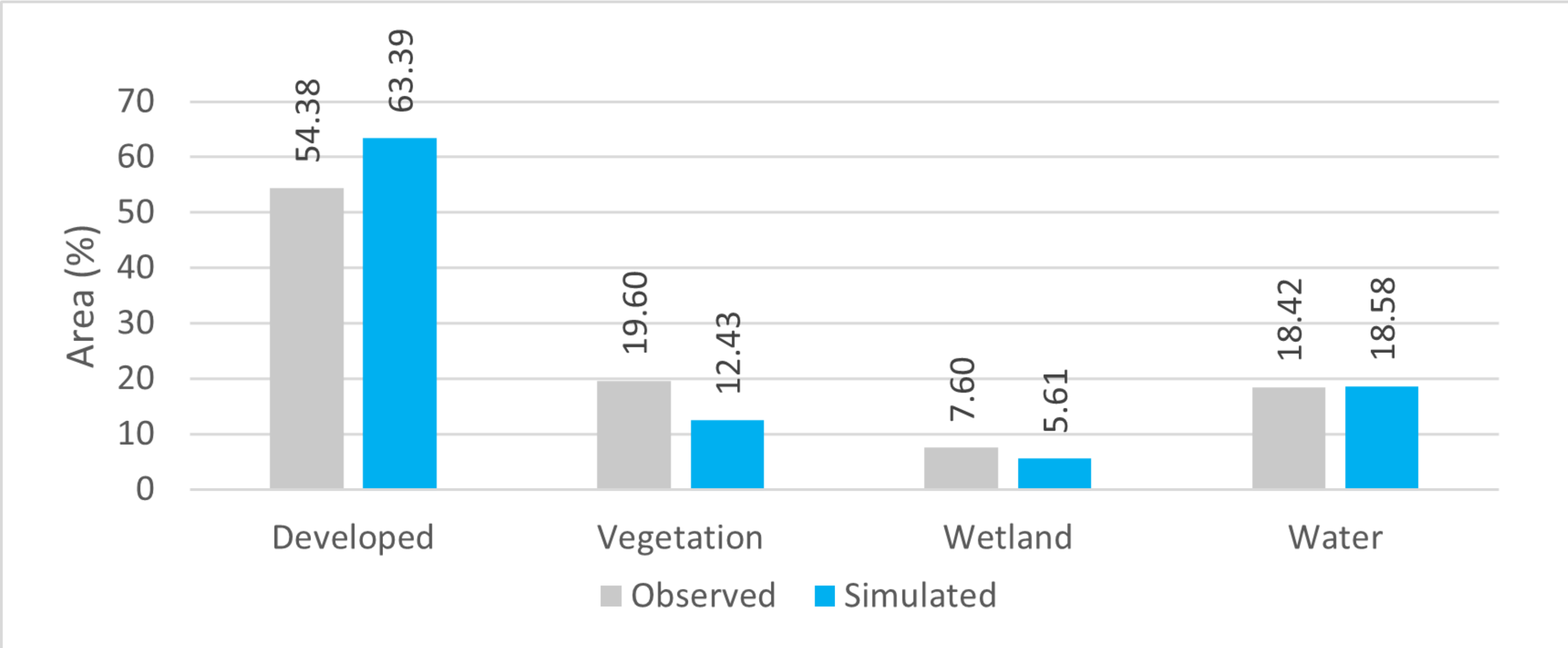

Figure 9. Statistical comparisons between simulated and observed LULC map for 2020

a)

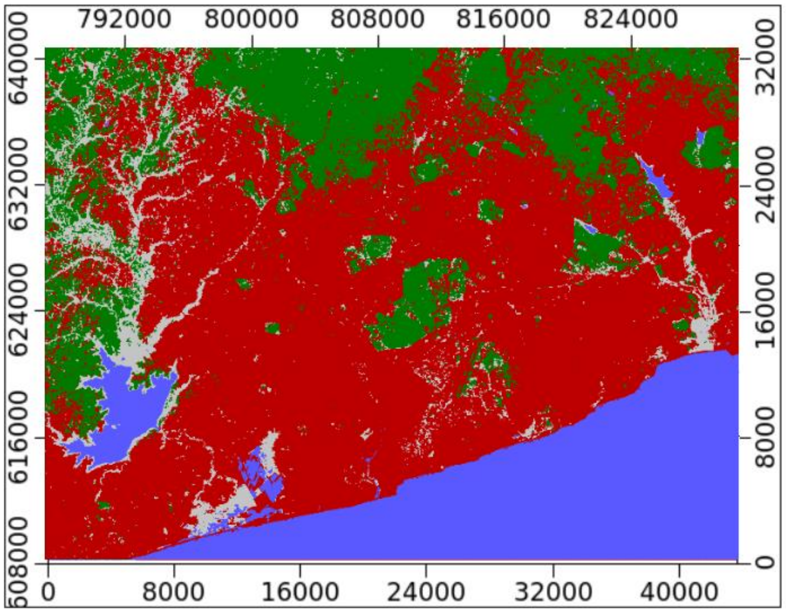

b)

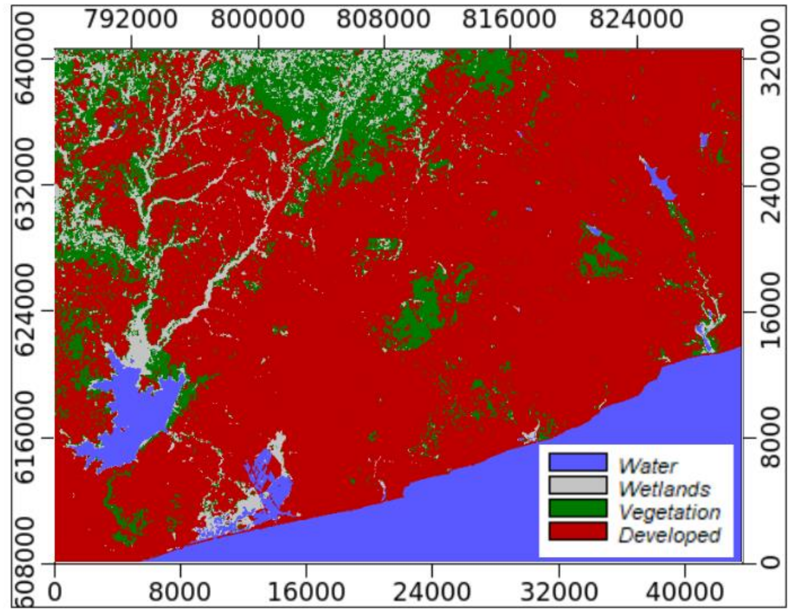

Figure 10. LULC maps for observed and predicted year 2020. (a) LULC map derived from Landsat images (b) simulated LULC map using CA-ANN model

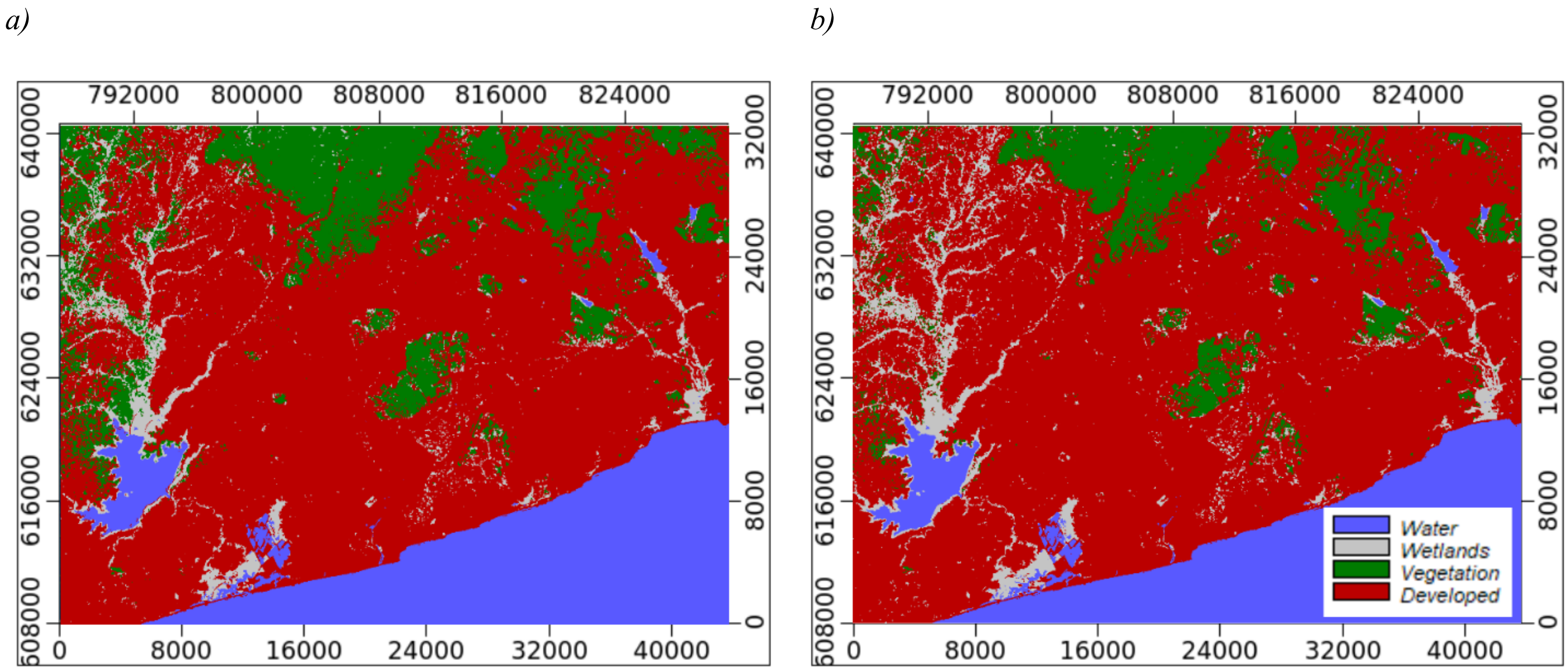

Figure 11. Simulated LULC maps for years (a) 2030 and (b) 2040

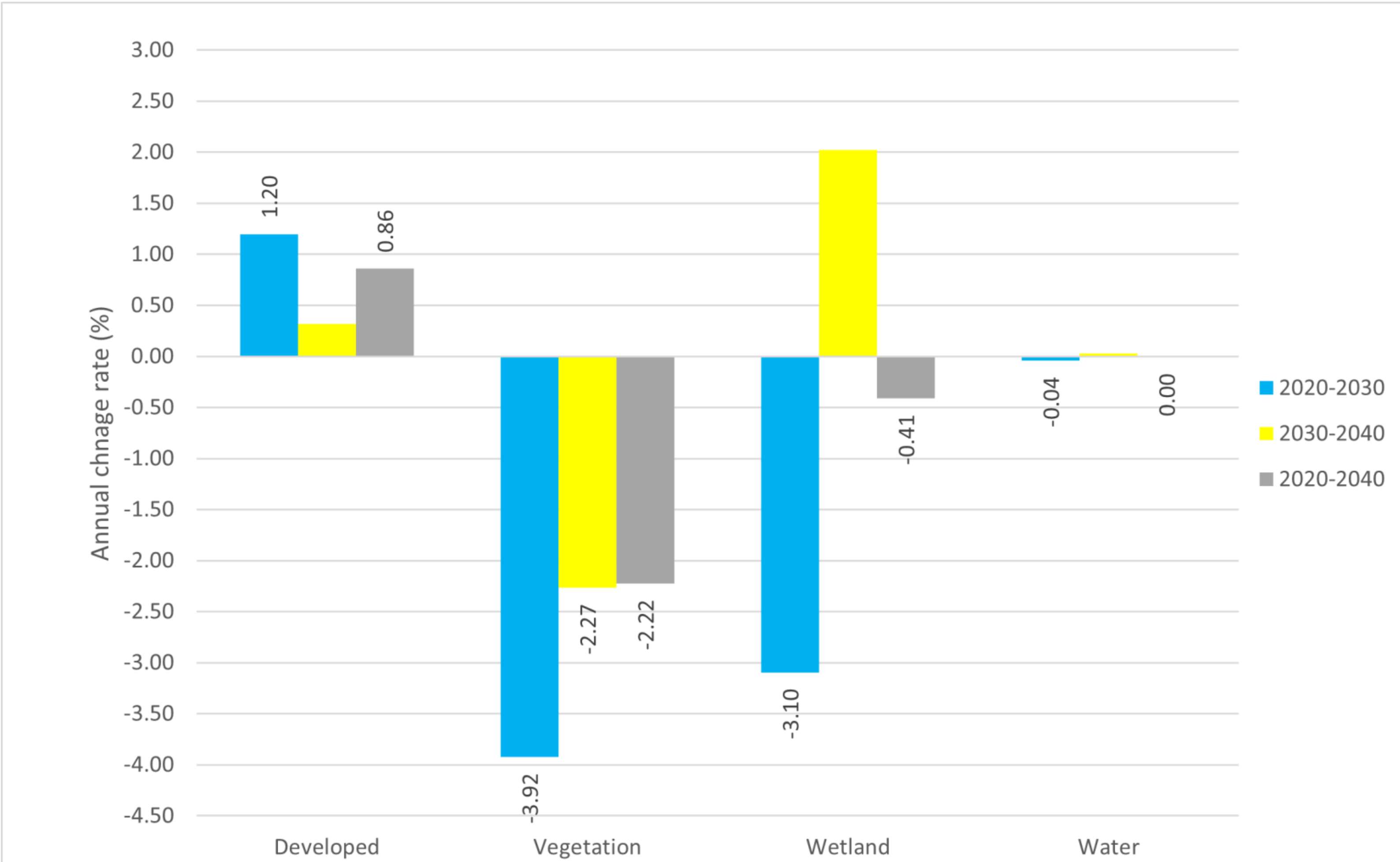

Figure 12. Annual change rate for future LULC for different time periods

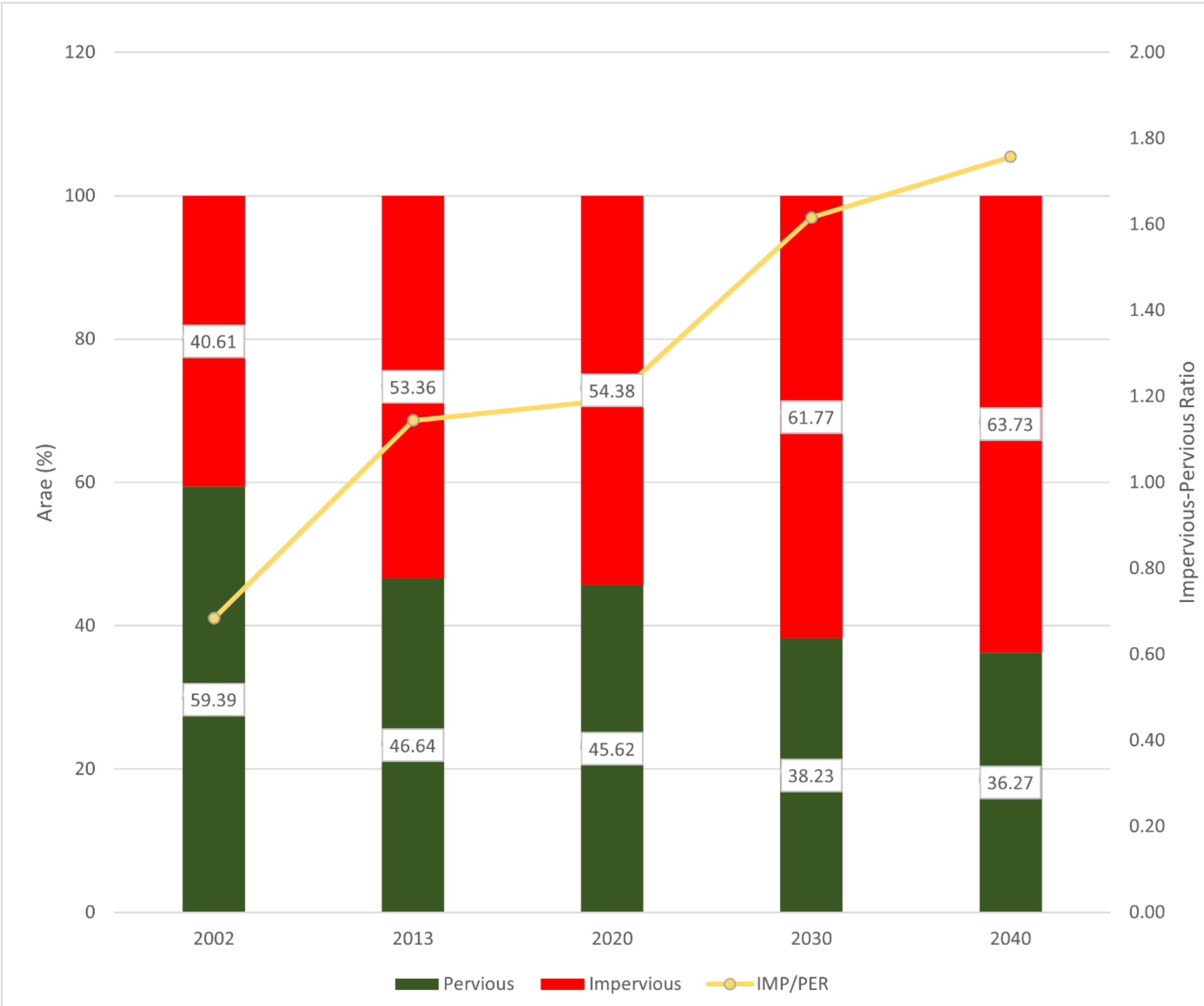

Figure 13. Impervious and pervious dynamics from 2002-2040

APPENDIX B TABLES

Table 1. Properties and characteristics of Landsat images.

Acquisition Date	Path/Row	Landsat Sensor	Spatial Resolution (m)	Number of Bands
12/26/2002	193/056	Landsat ETM+	30	7
01/06/2013	193/056	Landsat ETM+	30	7
01/02/2020	193/056	Landsat OLI	30	9

Table 2. Land cover classification scheme.

LULC Classes	Class Description
Developed	Residential, commercial and services, industrial, transportation, roads, mixed urban, and other urban, Exposed soils, construction sites, Transportation facilities
Vegetation	Deciduous forest, mixed forest lands, palms, conifer, scrub, cultivated land, crop fields, fallow lands, vegetable fields, Forest reserves, Herbaceous vegetation, Shrub and bush areas, Mixed grassland with few scattered trees, and others
Wetland	Permanent and seasonal wetlands, inland water bodies, low-lying areas, marshy land, rills, and gully, swamps
Water	River networks, canals, and active hydrological features

Table 3. Overall and kappa statistics

Year	Overall Accuracy	Kappa Coefficient
2002	0.93	0.91
2013	0.92	0.89
2020	0.94	0.92

Table 4. Producer and user accuracy for each LULC

Class	2002		2013		2020	
	Producer Accuracy	User Accuracy	Producer Accuracy	User Accuracy	Producer Accuracy	User Accuracy
Developed	96	97.00	97	99.00	93	95.00
Vegetation	88	91.00	84	91.00	96	95.00
Wetland	90	86	89	79	88	93
Water	98	98.00	98	100.00	99	100.00

Table 5. LULC changes (km²) and annual rate (%) for different time periods

Class	2002-2013		2013-2020		2002-2020		DD % between different time periods		
	Δ Area (sq. km)	Δ %	Δ Area (sq. km)	Δ %	Δ Area (sq. km)	Δ %	2002-2013	2013-2020	2002-2020
Developed	180.01	12.75	14.43	1.02	194.45	13.77	2.85	0.27	1.88
Vegetation	-182.45	-12.92	-39.27	-2.78	-221.72	-15.70	-3.33	-1.78	-2.47
Wetland	-2.82	-0.20	27.21	1.93	24.39	1.73	-0.31	4.85	1.63
Water	5.26	0.37	-2.37	-0.17	2.89	0.20	0.19	-0.13	0.06

Table 6. Transition probability statistics of LULC for 2002-2013

Classes	**Developed**	**Vegetation**	**Wetland**	**Water**
	2002-2013	2002-2013	2002-2013	2002-2013
Developed	0.926	0.064	0.005	0.005
Vegetation	0.416	0.494	0.091	0.000
Wetland	0.174	0.400	0.384	0.043
Water	0.004	0.000	0.001	0.994

Table 7. Transition probability statistics of LULC for 2002-2020

Classes	Developed	Vegetation	Wetland	Water
	2002-2020	2002-2020	2002-2020	2002-2020
Developed	0.901	0.068	0.025	0.006
Vegetation	0.455	0.443	0.102	0.001
Wetland	0.274	0.203	0.494	0.029
Water	0.007	0.000	0.005	0.988

Table 8. Different combinations of spatial variables and kappa coefficients

Driver Combination	Percentage of Correctness	Kappa Coefficients
Road, River, Town, Slope	79.10	0.66
River, Town, Slope, Elevation	77.83	0.64
Road, River, Town, Elevation	78.67	0.64
Road, River, Slope, Elevation	77.93	0.63
Road, Town, Slope, Elevation	77.09	0.61
Road, River, Town, Slope, Elevation	78.50	0.70

Table 9. LULC distribution for future LULC and estimated annual change rate for 2020-2030,2030-2040 and 2020-2040

Class	2020	2030	2040	DD % between different time periods		
	Area (sq. km)	Area (sq. km)	Area (sq. km)	2020-2030	2030-2040	2020-2040
Developed	768.00	872.39	900.03	1.20	0.32	0.86
Vegetation	276.76	198.79	153.75	-3.92	-2.27	-2.22
Wetland	107.37	81.99	98.58	-3.10	2.02	-0.41
Water	260.14	259.10	259.91	-0.04	0.03	0.00